PETROCHEMISTRY OF EARLY CRETACEOUS POTASSIC ROCKS FROM THE ASUNCIÓN-SAPUCAI GRABEN, CENTRAL-EASTERN PARAGUAY

P.Comin-Chiaramonti, P.Censi, A.Cundari, A.De Min, C.B.Gomes, A.Marzoli, E.M.Piccirillo

Alkaline Magmatism in Central-Eastern Paraguay. Relationships with Coeval Magmatism in Brazil. Comin-Chiaramonti, P. & Gomes, C. B. (eds.), 1996, Edusp/Fapesp, São Paulo, pp. 123-150.

ABSTRACT

A comprehensive investigation of potassic rocks forming intrusive, lava and dyke bodies in central-eastern Paraguay was undertaken with the main aim of characterizing the rock associations in the context of the Early Cretaceous igneous activity in South America.

This study, based on an analytical data bank obtained from over 400 specimens, enabled to recognize two main suites, i.e. a basanite-tephrite-phonotephrite-phonolite (B-P) and an alkali basalt-trachybasalt-trachyandesite-trachyphonolite/trachyte (AB-T), respectively. Most compositions fall within the range 49-54 SiO_2 (wt %), only about 12% of the B-P rocks having SiO_2>54 (wt %). On the other hand, about 37% of the AB-T rocks yielded SiO_2>54 (wt %) with two maxima at 52 and 58, respectively. Compositions with K_2O/Na_2O=1-2 (K) are dominant, while compositions with K_2O/Na_2O>2 (HK) are important among the intrusive bodies and dykes. Transitional (tK) compositions, as defined by Comin-Chiaramonti et al. (this volume, Magmatism) are abundant in the dyke swarms, but subordinate and uniformely distributed in the B-P and AB-T suites (23% and 24%, respectively).

Intrusives, dykes and lavas show scattered compositions with similar chemical variations, suggesting that subsolidus transformations may have been important. Relatively low Cr and Ni (mean=320±83 ppm and 89±28 ppm, respectively) of the specimens with mg#>0.6 (N=62) indicate evolved liquid compositions and support the view that crystal fractionation was important in the evolution of the suites even for the compositions with highest mg# (0.63-0.73).

REE patterns display strong LREE fractionation. Strong LILE/HFSE fractionation and negative Ta-Nb-Ti anomalies mimic those of the associated tholeiitic basalts of the Serra Geral Formation. This important relationship and the geological setting of the province are not favourable to a subduction-driven magma genesis.

A garnet peridotite mantle source seems consistent with the petrochemical data to approach the problem of the origin and genesis of the suites.

INTRODUCTION

Previous studies of the alkaline magmatism in Eastern Paraguay mainly focussed on the central region (i.e. the Asunción-Sapucai graben, ASU; Fig.1), where shallow level intrusives, thick flow sequences and dykes are well exposed and close to the main roads (Gomes et al., this volume).

A systematic petrological study of the above region was initially undertaken by an international team from the Universities of São Paulo

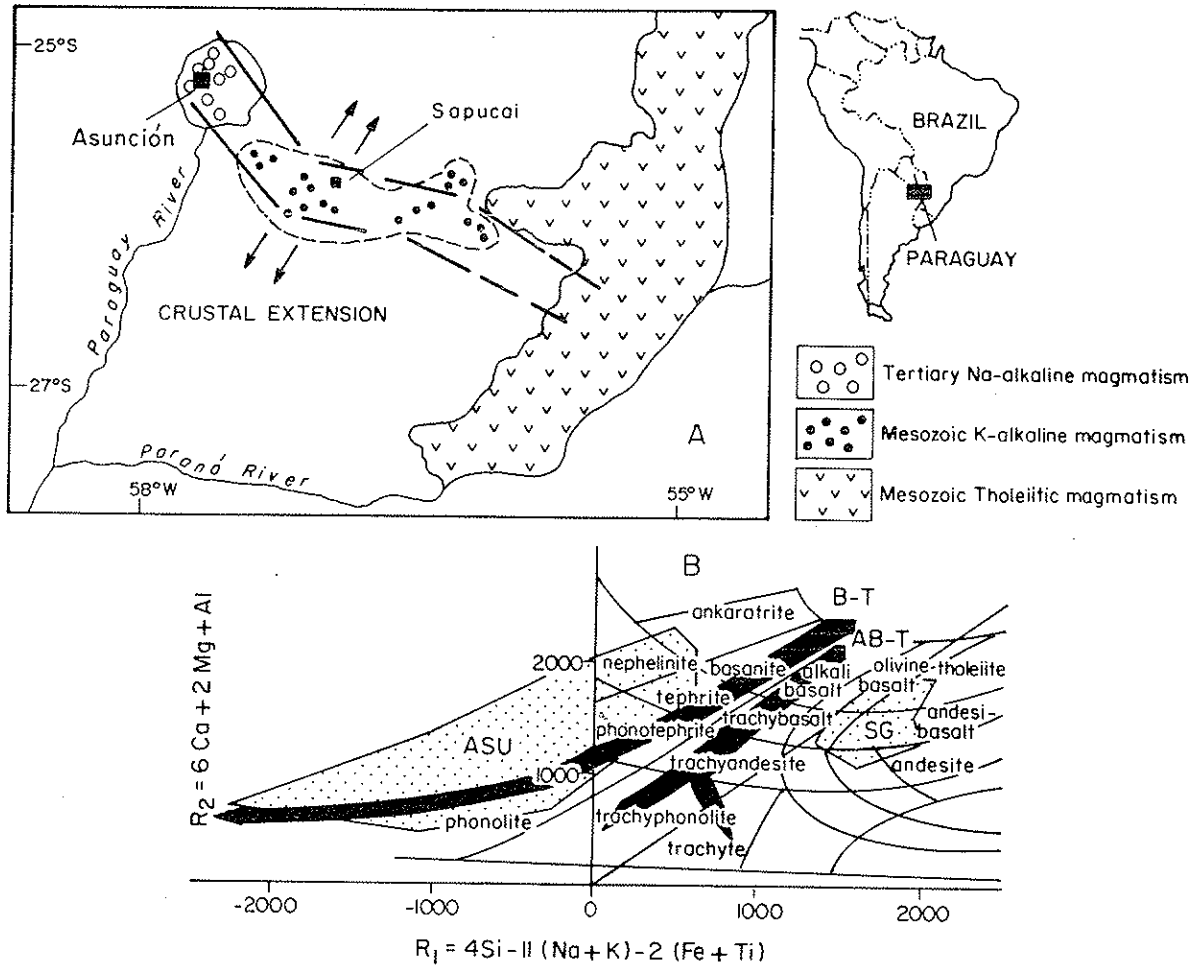

Figure 1 - A. Map of the Asunción-Sapucai graben, showing the major outcrops of igneous rocks. B. R1-R2 plot (De La Roche et al., 1980) with the fields of the tholeiitic (SG) and alkaline (sodic) rocks (ASU) from Eastern Paraguay and the general trends of the B-P and AB-T suites (nomenclature of lavas only is shown). Data source: Bellieni et al., 1986; Comin-Chiaramonti et al., 1991; Comin-Chiaramonti et al. (this volume, Appendix II).

Melbourne (Australia) and Asunción (Paraguay), with the main aim of understanding the genetic relationships between the dominant continental flood basalts of the Serra Geral Formation and the associated alkaline rocks in western Gondwana. This is fundamental in understanding the relationship between magmatic activity and the opening of the South Atlantic Ocean.

This paper presents the results of a comprehensive petrochemical investigation of the potassic rocks in central-eastern Paraguay with the view of delineating their elemental distribution and variations in terms of their occurrence and distribution, i.e.intrusive, lava flow and dyke formations. Two suites were recognized, i.e. basanite-tephrite-phonotephrite-phonolite (B-P) and alkali basalt-trachybasalt-trachyandesite-trachyphonolite/trachyte (AB-T), respectively (Comin-Chiaramonti et al., this volume, Magmatism). The data base is given in Comin-Chiaramonti et al. (this volume, Appendix II).

Major and trace element analyses were carried out at Trieste University (Italy) by P. Comin-Chiaramonti, A. De Min and A. Marzoli, using the XRF procedures described in Bellieni et al. (1983). Major element compositions were recalculated to 100%, on an water-free basis, total Fe being given as FeO. REE, Th, U, Ta and Y of selected specimens were measured by a Perkin-Elmer Sciex Elan 500 mass spectrometer (ICPM) at CEPA s.r.l. (Palermo, Italy), following the procedure described by Alaimo & Censi (1992).

FREQUENCY DISTRIBUTION

The SiO_2 (wt %) frequency distribution of potassic rocks shows that the specimens of the B-

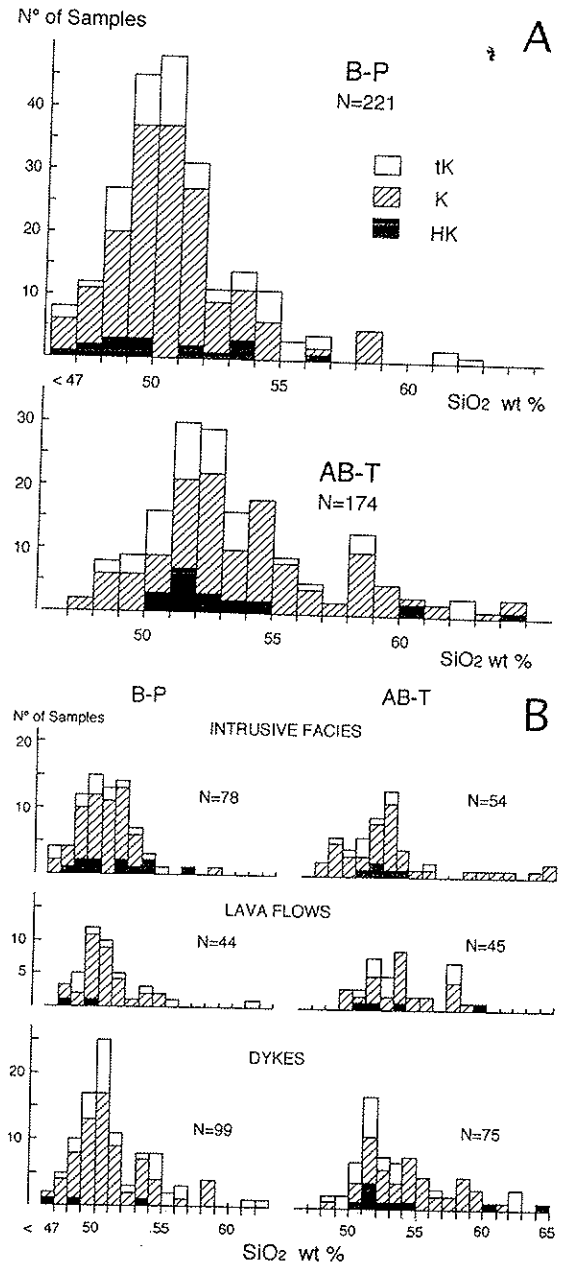

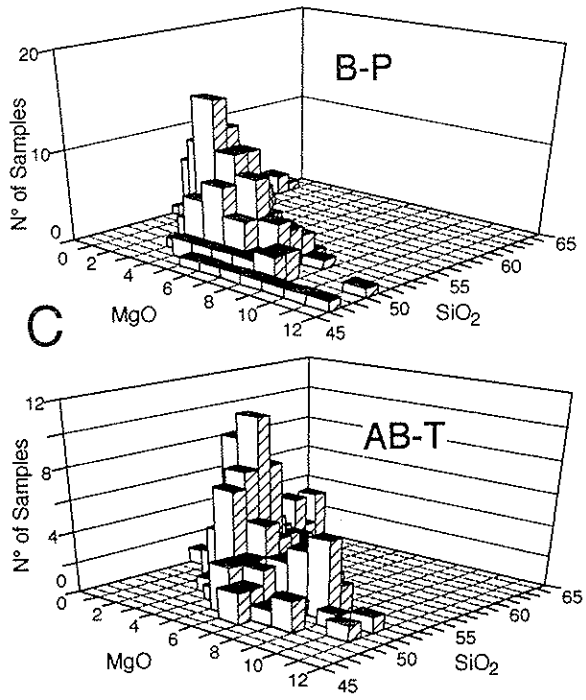

Figure 2 - A. SiO_2 (wt %) histograms for basanite/tephrite/phonotephrite/phonolite (B-P) and alkali basalt/trachybasalt/trachyandesite (AB-T) suites. HK: $K_2O/Na_2O \geq 2$; K: $(2<K_2O/Na_2O<1)$; tK: $(K_2O/Na_2O<1)$. B. histograms subdivided into intrusives, lavas and dykes. C. insets: histograms showing frequency distribution for SiO_2 vs. MgO (wt %) for the B-P and AB-T suite, respectively.

P suite yielded a maximum between 49 and 51 wt %, and those of the AB-T suite between 51 and 53 wt % (Fig. 2A). The SiO_2 frequency distribution of the B-P suite is probably unimodal, owing to the scarce number (c. 12%) of specimens with silica in the 54-63 wt % range.

The specimens of the AB-T suite tend to concentrate at SiO_2>54 wt % (37%) and form a bimodal distribution, due to the "high" represented by rocks with SiO_2 in the 58-59 wt % range (7.5%; Fig. 2A).

Compositions with K_2O/Na_2O wt % ratio in the 1-2 range (K group; Comin-Chiaramonti et al., this volume, Magmatism) are dominant. Transitional compositions (Na_2O-2$\leq K_2O$ to $K_2O/Na_2O \leq 1$: tK group) are subordinate and uniformely distributed (23% and 24% in the B-P and AB-T suite, respectively). Compositions with K_2O/Na_2O>2 (HK group) prevail among the intrusives, while tK are abundant in the dyke swarm.

Total alkali distribution (Na_2O+K_2O wt %) is unimodal in both suites (Fig. 3A), with a tendency of the specimens from the B-P suite toward higher (Na_2O+K_2O) values {47% of specimens with (Na_2O+K_2O)>9 wt %} relative to those from the AB-T suite {35% of specimens with (Na_2O+K_2O)>9 wt %}.

Generally, the specimens from the latter suite are also lower in Na_2O relative to those of the B-P suite.

Compared with specimens with $SiO_2 \leq 54$ wt%, it is apparent that specimens from the B-P and AB-T suites average similar SiO_2 and Na_2O values (SiO_2=50.19±2.02 wt %, Na_2O=3.80± 1.02 wt %; and SiO_2= 51.67± 1.70 wt %, Na_2O =3.33±1.02 wt %, respectively). However, the specimens from the AB-T suite (Figs. 3B and 3C) are grouped toward lower TiO_2 (1.54±0.27 wt

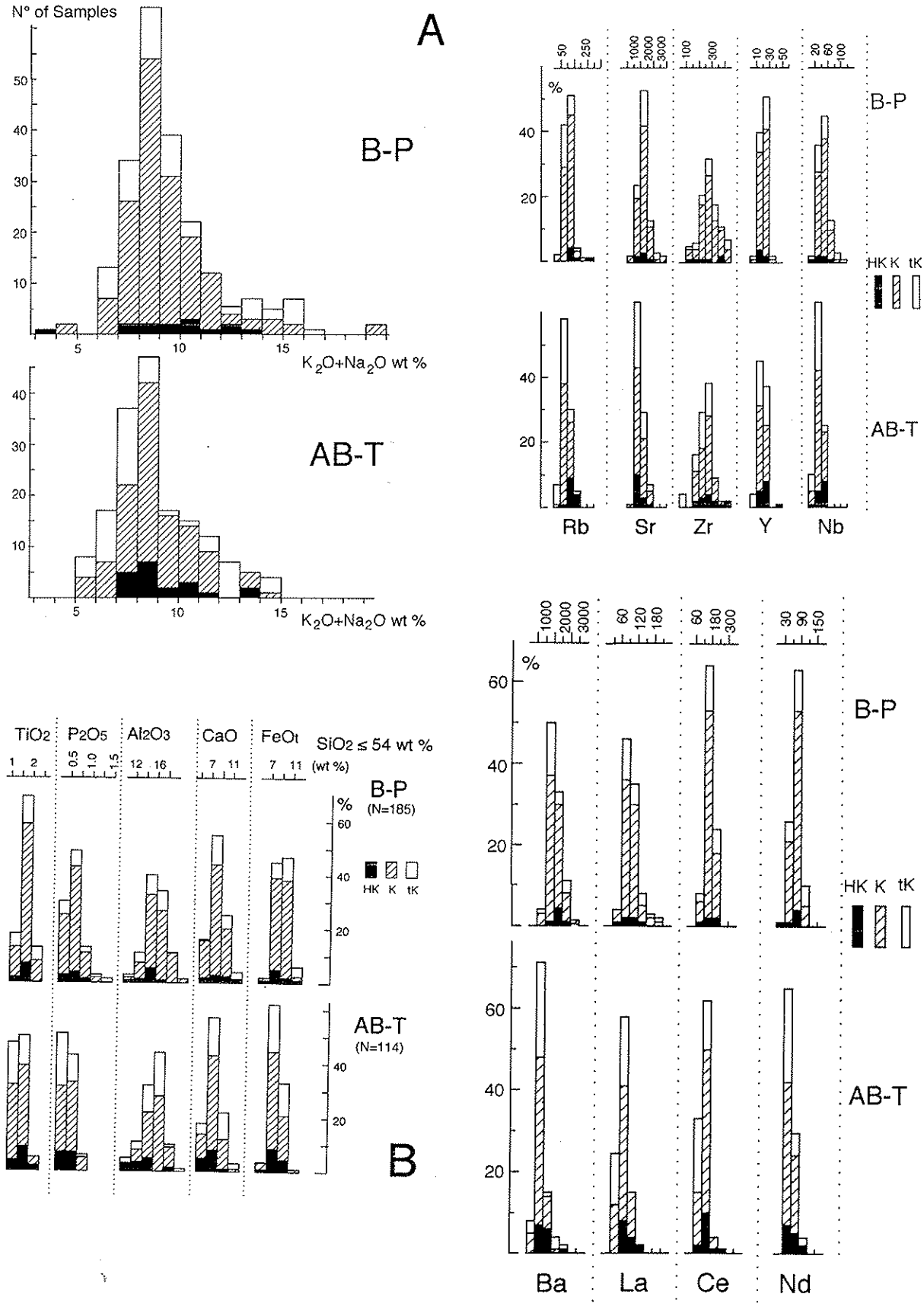

Figure 3 - A. Histograms of Na_2O+K_2O (wt %) for B-P and AB-T compositions; B. TiO_2, P_2O_5, Al_2O_3, CaO and FeO total for $SiO_2 \leq 54$ wt %; C. trace elements (ppm) for $SiO_2 \leq 54$ wt %. Symbols and ornaments as in Fig. 2.

%), P_2O_5 (0.51±0.13 wt %) and incompatible elements (ppm: Rb=92±32, Sr=1477±333, Zr=243±64, Y=19±5, Nb=32±11, Ba=1354± 405, La=74±22, Ce=132±34, Nd=56±14) than those from the B-P suite (i.e. TiO_2=1.68±0.32 wt % and P_2O_5=0.59±0.20 wt %; Rb=103±49, Sr=1722±440, Zr=291±88, Y=21±6, Nb=45± 17, Ba=1523±392, La=92±25, Ce=162±40, Nd=68±16 ppm).

Average compositions of specimens with $SiO_2 \leq 54$ wt % from both the B-P and AB-T suites, representing intrusives, lavas, and dykes are given in Table 1.

VARIATION DIAGRAMS

The compositional variation of the alkaline rocks relative to SiO_2 wt % is shown in Figures 4 to 9.

In general, Al_2O_3, Na_2O and K_2O increase and CaO, FeO_t, MgO, TiO_2 and P_2O_5 decrease as SiO_2 increases, while the trace elements are widely scattered.

It is evident that the compositional ranges result from the presence of two main groups, i.e. B-P and AB-T suites, respectively, whose compositional fields partially overlap.

Comparing strongly compatible elements, e.g. Cr and Ni, and strongly incompatible elements, e.g. Zr, it can be inferred that the initial zirconium values (Zr_0) should be in the range 100-400 ppm for both B-P and AB-T suites (average: Zr_0=291 and 243 for B-P and AB-T, respectively; cf. Figs. 10 and 11 and Table 1), suggesting evolution of liquids from different parental sources.

Notably, correlations between Zr and other incompatible elements, particularly Nb, La, Ce, Nd, for both suites are not in general represented by straight lines passing through the origin.

However, the high positive correlations, between Zr and other incompatible elements e.g. LREE (cf. regression lines of Figs. 10 and 11), discriminate well the B-P from the AB-T compositions, suggesting liquid evolution at roughly constant LREE/Zr ratios.

Wide scattering of points is observed in the most evolved compositions i.e. trachytes, trachyphonolites and phonolites and their intrusive equivalents.

Y is strongly scattered in the B-P compositions, while there is a rough correlation with Zr ($r \sim 0.74$) in the AB-T compositions with $SiO_2 \leq 54$ wt %.

In both suites, some of the peralkaline compositions have very low Y and relatively high Zr, suggesting possible garnet fractionation (Ti-andradite; cf. Cundari & Comin-Chiaramonti, this volume; Comin-Chiaramonti et al., this volume, Appendix III), and very high fO_2 conditions.

RARE EARTH (REE) AND INCOMPATIBLE ELEMENTS (IE)

REE and IE variations of representative samples are presented in Table 2. Chondrite-normalized REE plots for intrusives, lavas and dykes of the B-P and AB-T suites are illustrated in Figures 12 and 13, respectively.

All rock-types are strongly enriched in REE and exhibit steep chondrite normalized profiles (La: 21-164 and 33-157 ppm, La_N/Lu_N: 26-161 and 17-62, B-P and AB-T suites, respectively). The analyzed samples yielded similar parallel to subparallel trends which tend to flatten out in the HREE (Dy_N/Lu_N: 1.24-1.96 and 1.09-2.00, B-P and AB-T, respectively), except for two samples of the B-P suite, i.e. 2-HK and 10-HK (Table 2A), representing a seriate essexite, and a xenolith of essexitic gabbro with cumulate leucite + biotite + alkali feldspar, respectively.

The latter two samples display the highest Dy_N/Lu_N ratios (6.61 and 7.55, respectively), showing also the lowest and highest REE concentrations, respectively (Table 2A and Fig. 12).

Excluding cumulate assemblages (e.g. 2-HK; Table 2A), Eu/Eu* tends to show scattered negative values in the B-P group (0.86±0.14) against the "normal" values of the AB-T group (Eu/Eu* = 0.96±0.08).

The similarity in REE profiles suggests that all the potassic rocks reflect similar processes and the high LREE/HREE ratios imply that garnet may have been a residual phase in their generation.

Differences between intrusions may reflect slight variations in degree of melting and/or different metasomatized sources (cf. also Comin-Chiaramonti et al., 1992).

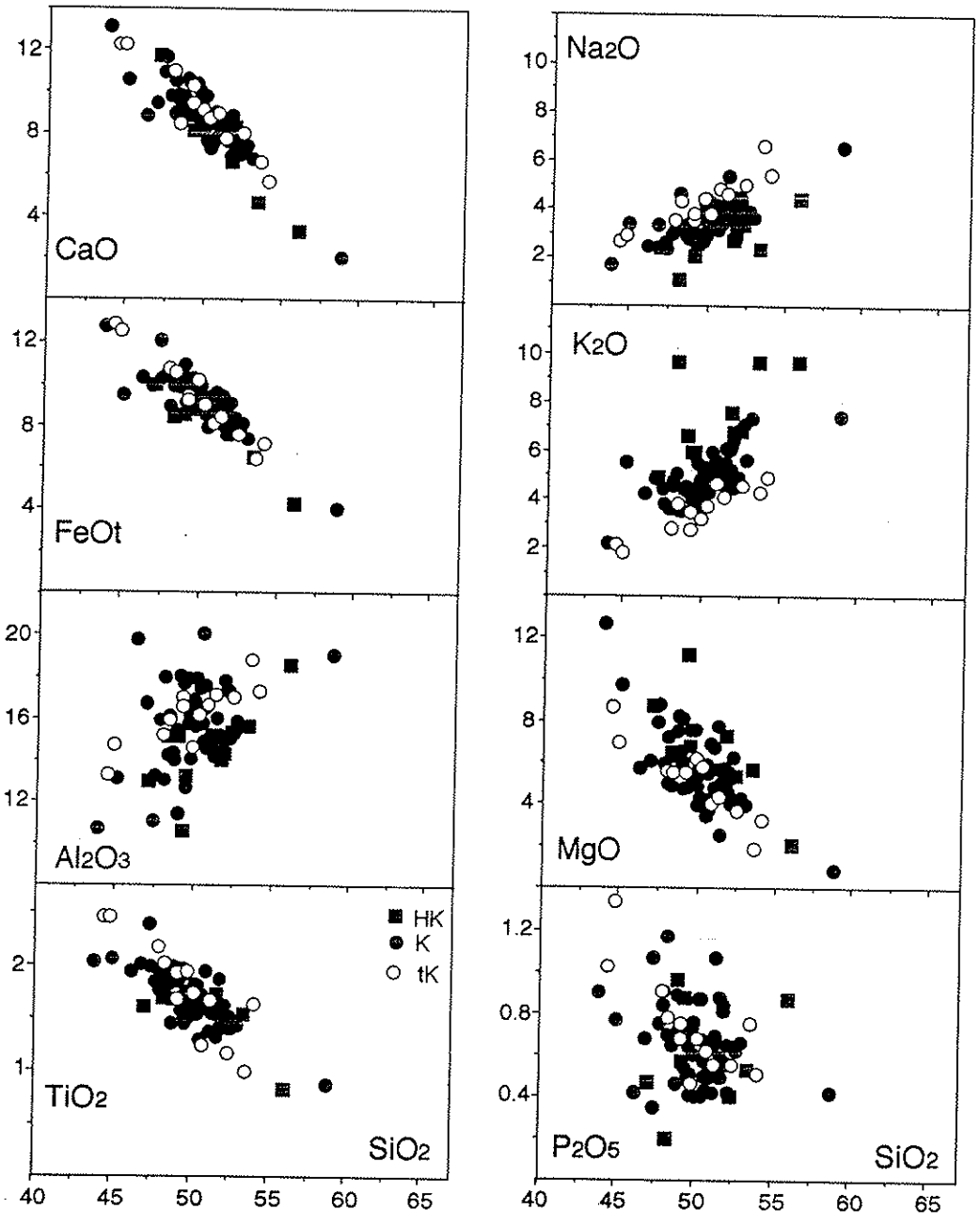

Figure 4A - SiO_2 vs. major elements (wt %) for intrusives of the B-P suite. Squares, full circles and open circles: HK (highly potassic), K (potassic), and tK (transitional potassic) groups, respectively (cf. Comin-Chiaramonti et al., this volume, Magmatism).

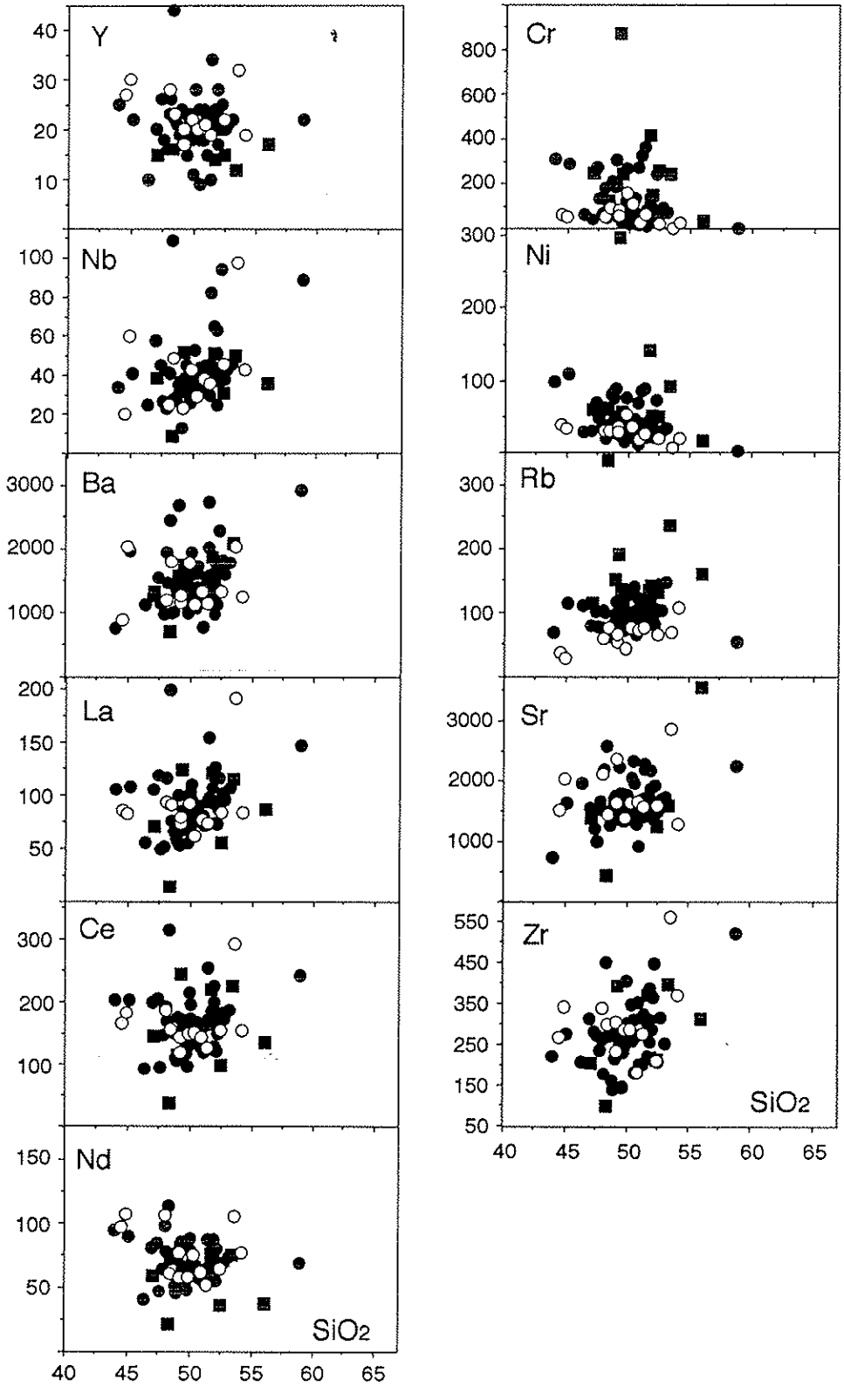

Figure 4B - SiO_2 (wt %) vs. trace (ppm) elements for intrusives of the B-P suite. Symbols as in Fig. 4A.

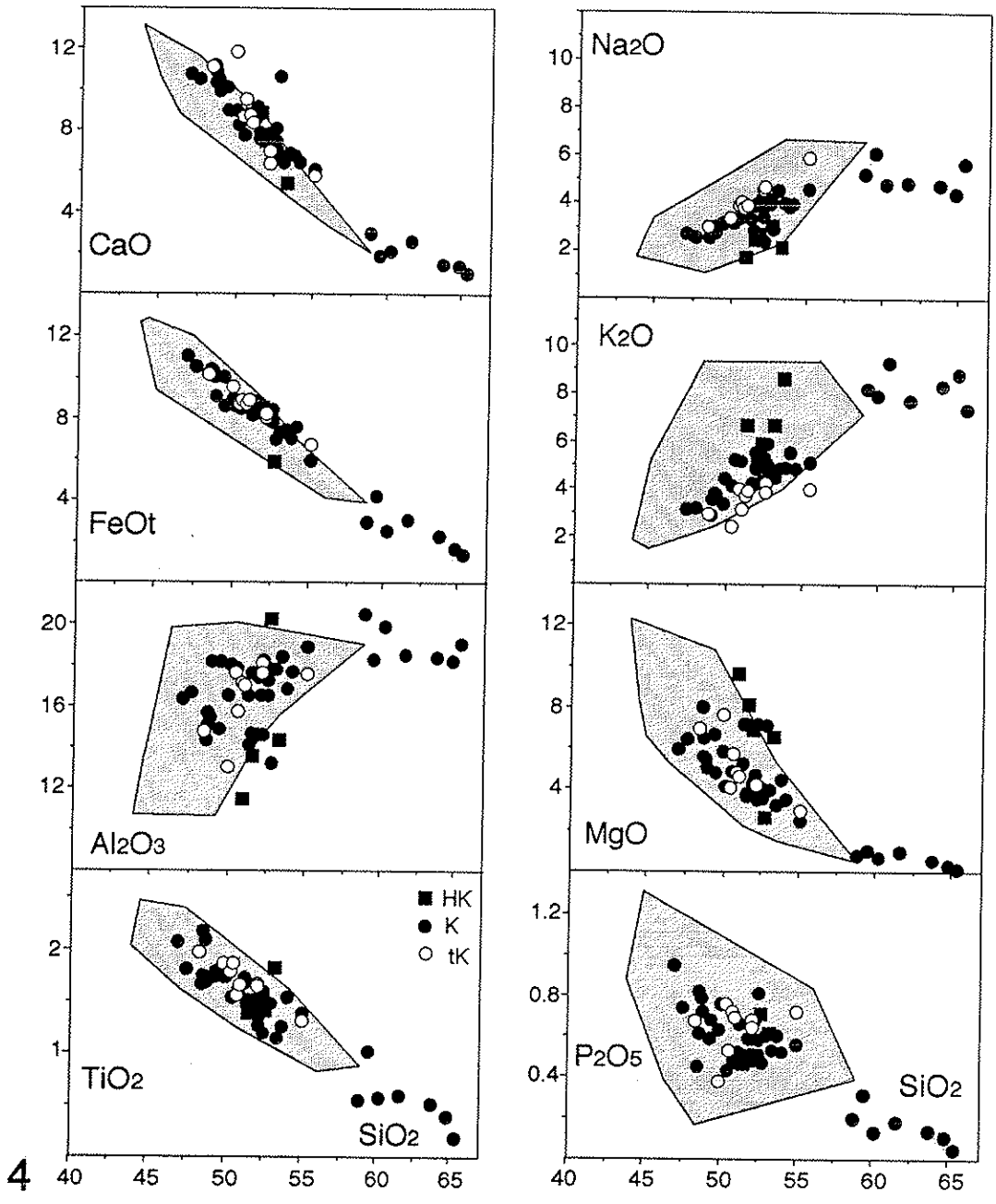

Figure 5A - SiO_2 vs. major elements (wt %) for intrusives of the AB-T suite. Dotted area: variation of the B-P suite. Other symbols as in Fig. 4A.

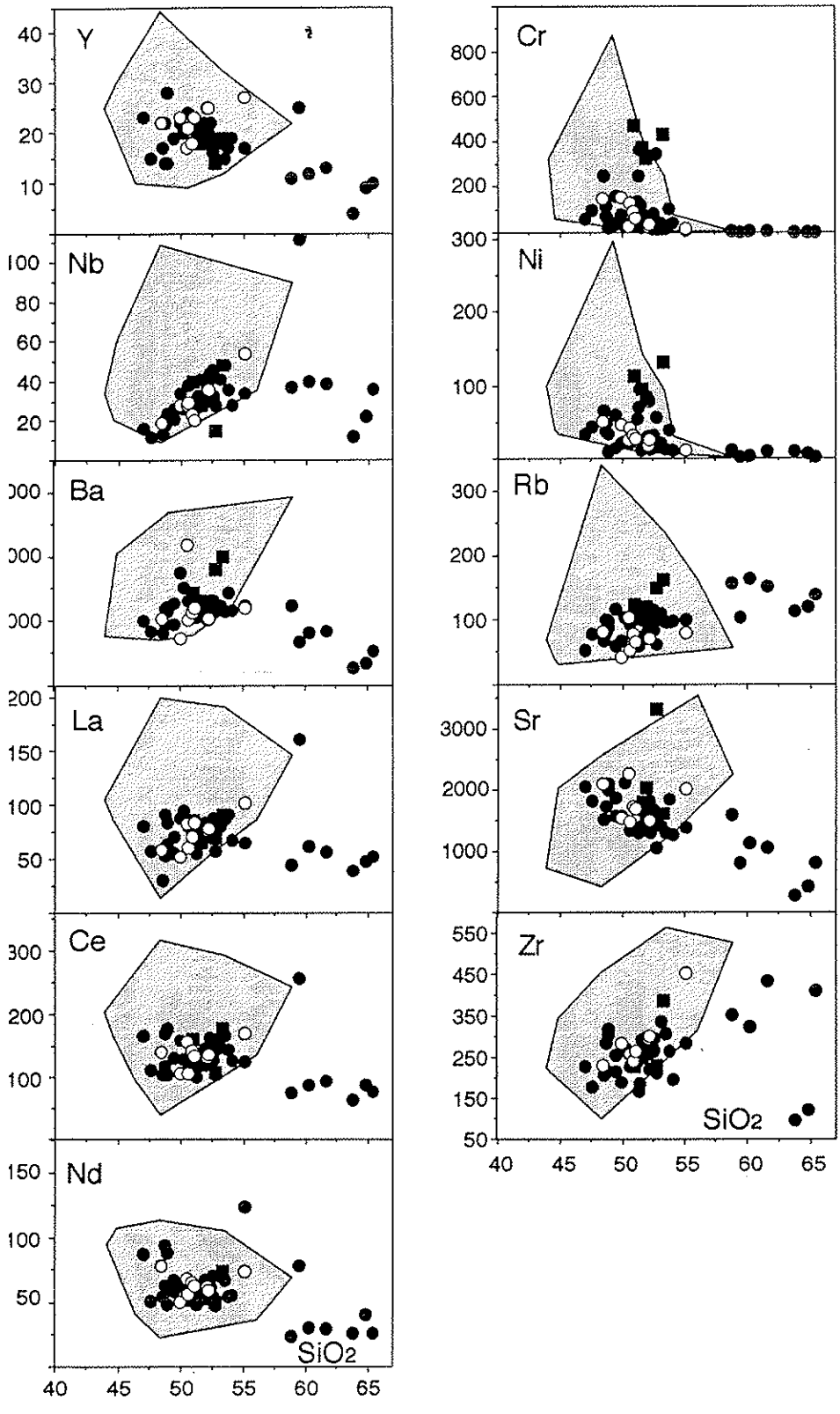

Figure 5B - SiO_2 (wt %) vs. trace (ppm) elements for intrusives of the AB-T suite. Dotted area: variation of the B-P series. Other symbols as in Fig. 4A.

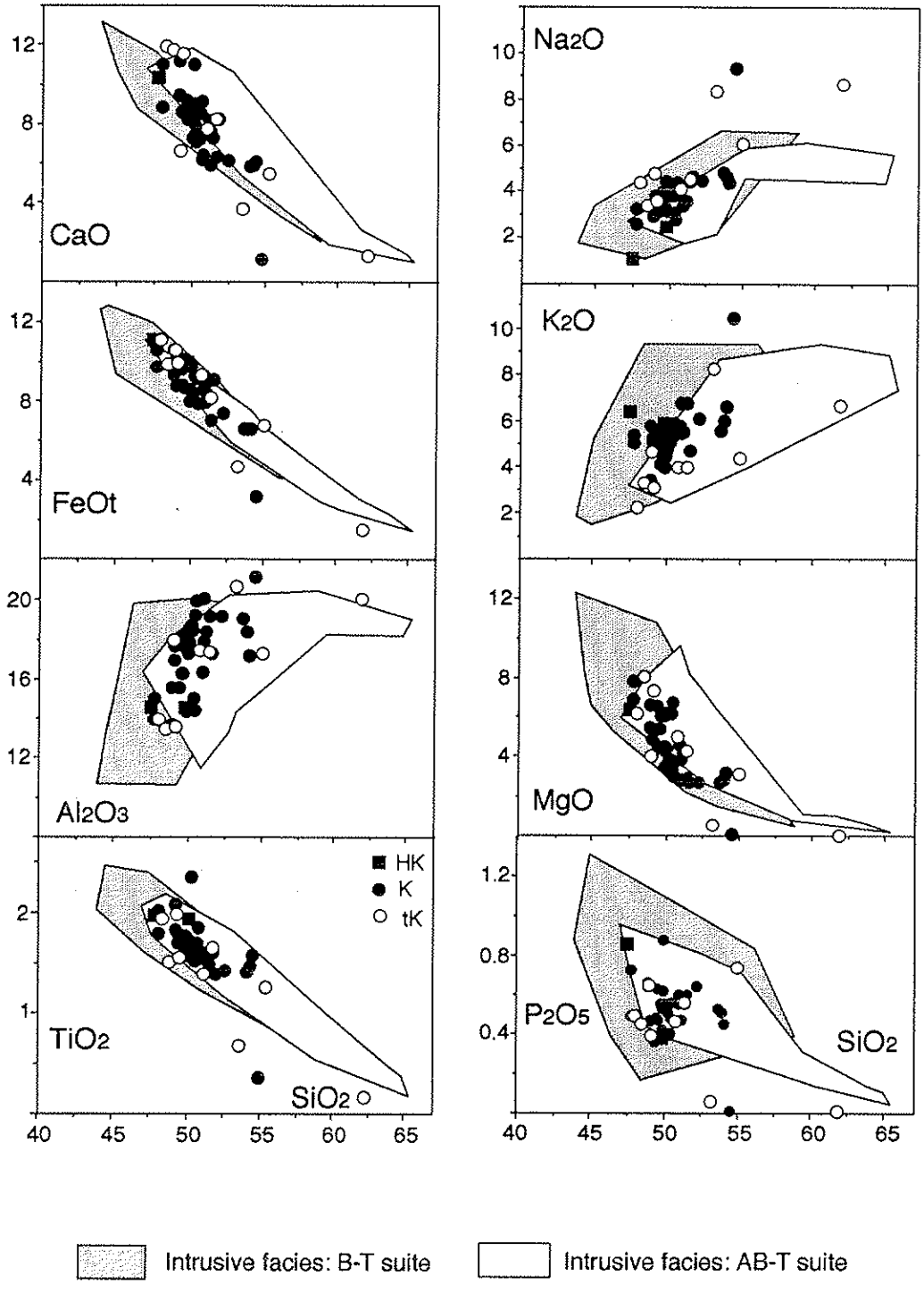

Figure 6A - SiO_2 vs. major elements (wt %) for lavas of the B-P suite. Symbols and ornaments as in Fig. 4A.

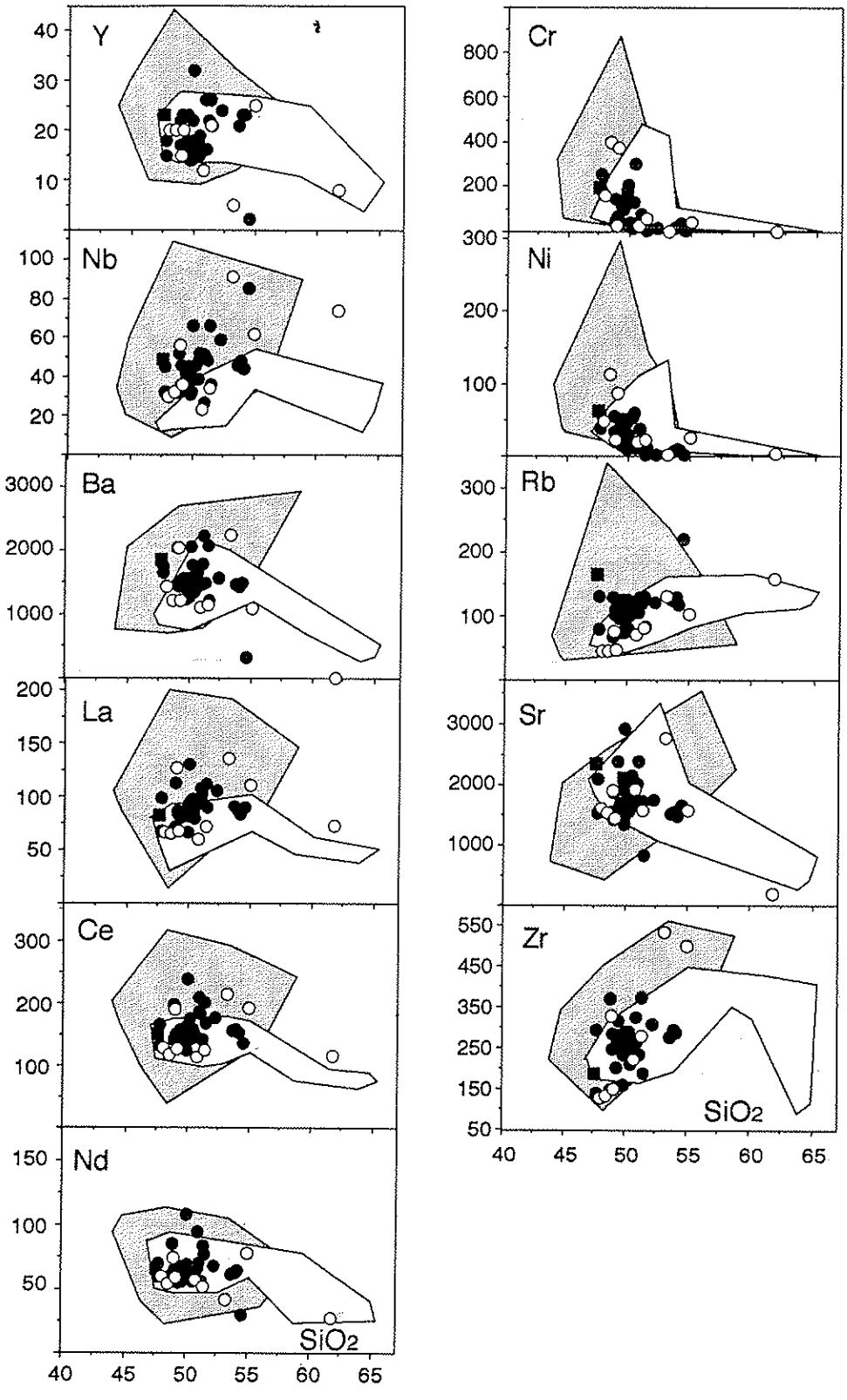

Figure 6B - SiO_2 (wt %) vs. trace (ppm) elements for lavas of the B-P suite. Other symbols as in Fig. 4A.

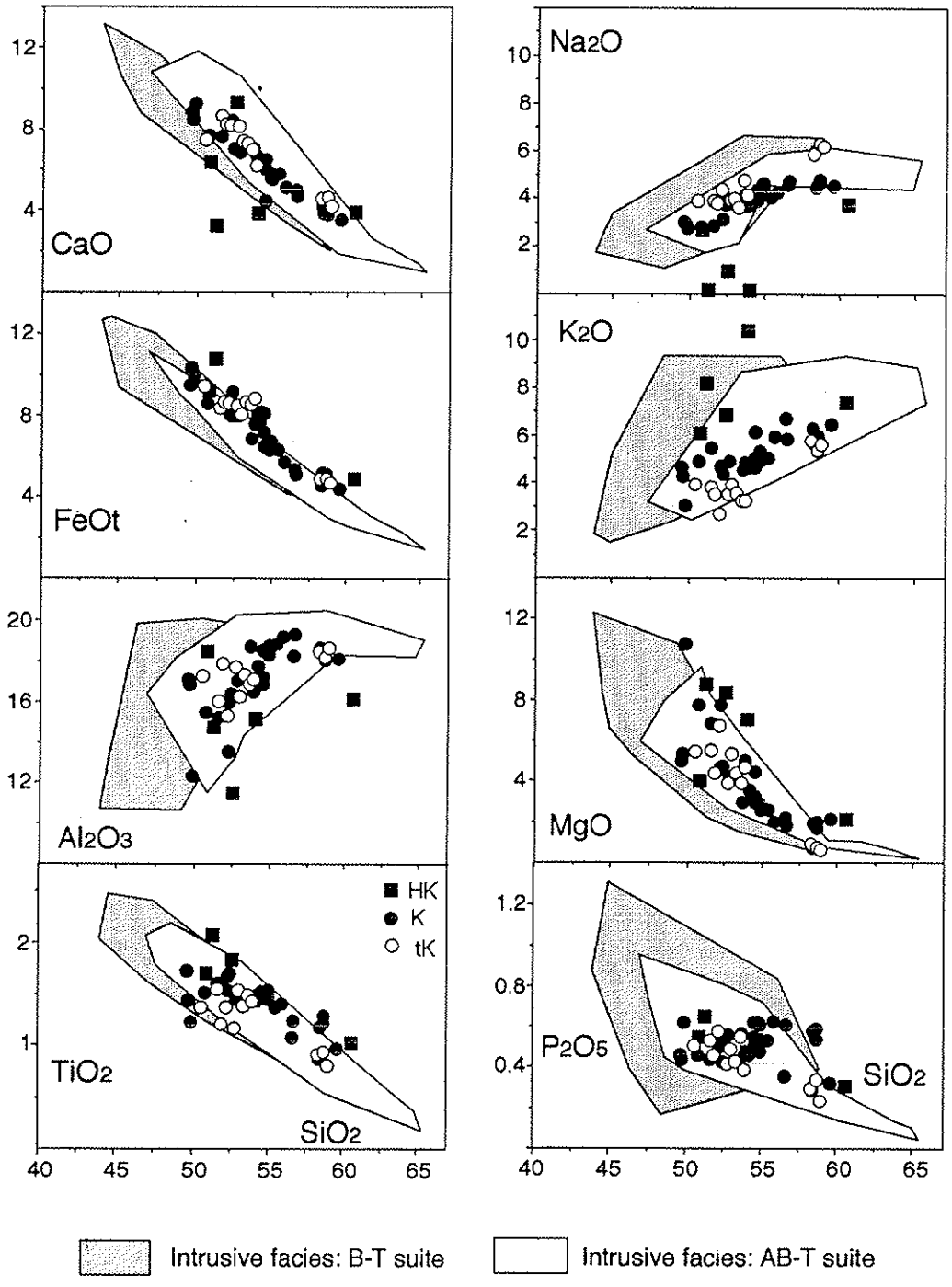

Figure 7A - SiO_2 vs. major elements (wt %) for lavas of the AB-T suite. Symbols as in Fig. 4A.

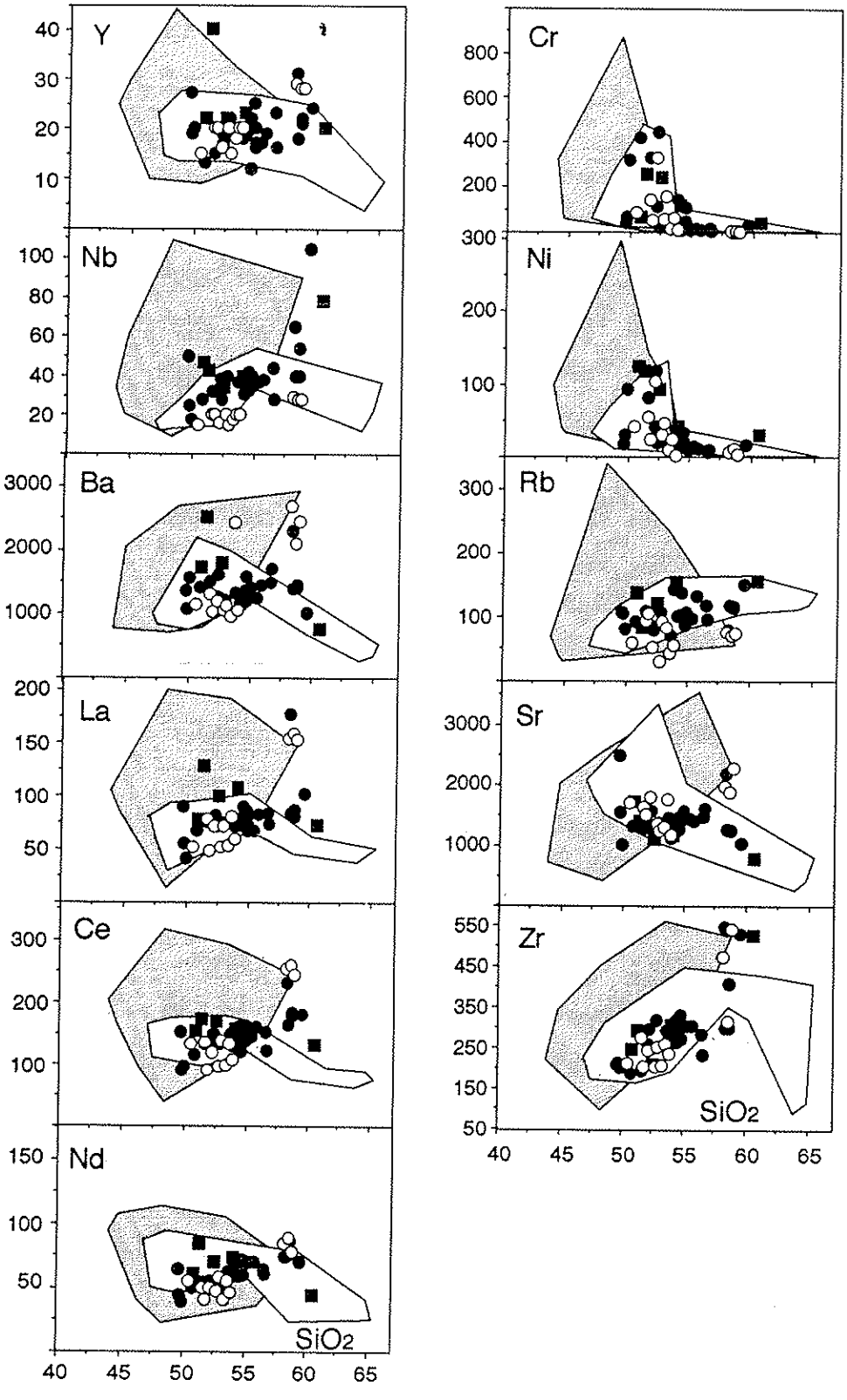

Figure 7B - SiO_2 (wt %) vs. trace (ppm) elements for lavas of the AB-T suite. Other symbols as in Fig. 4A.

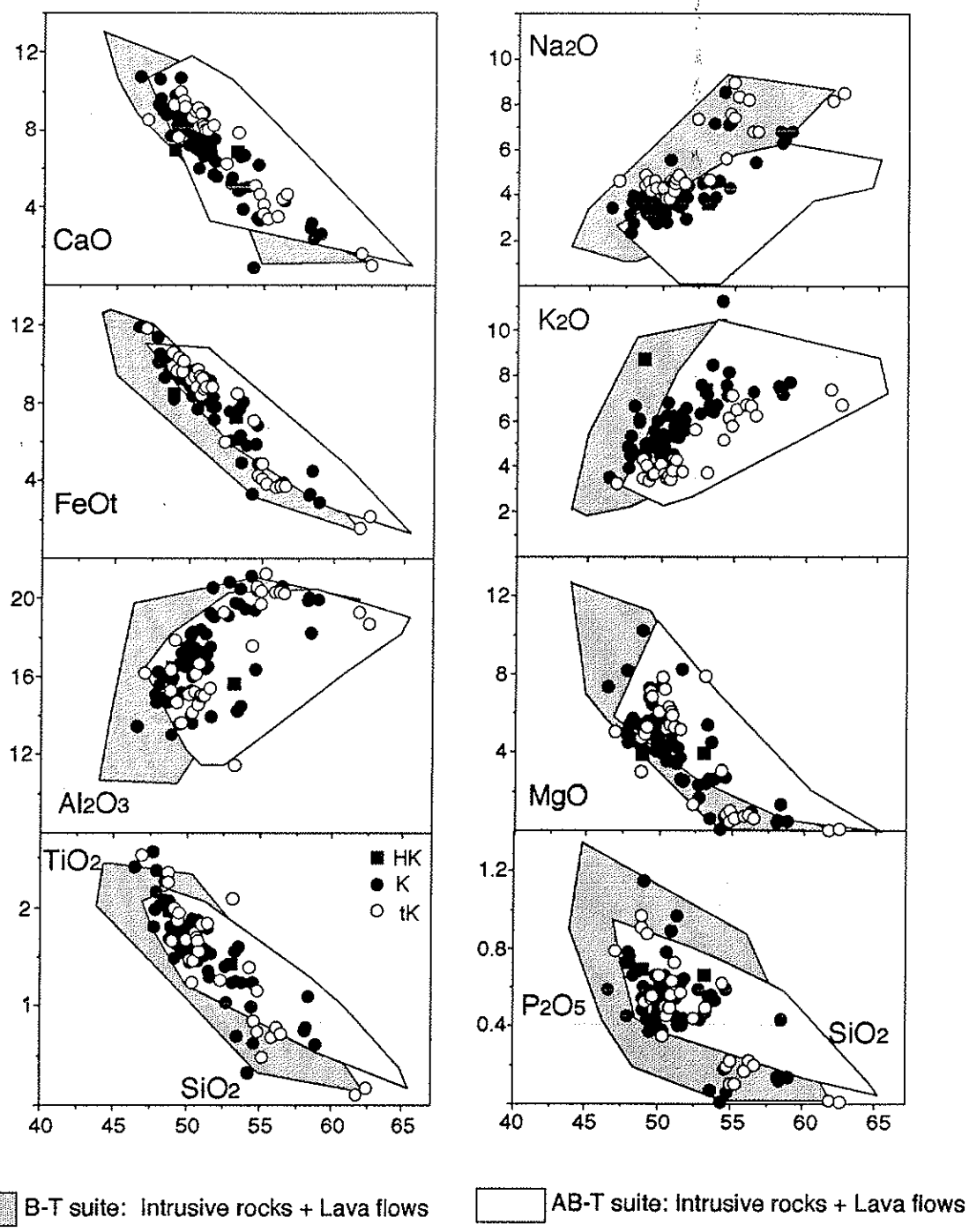

Figure 8A - SiO_2 vs. major elements (wt %) for dykes of the B-P suite. Symbols as in Fig. 4A.

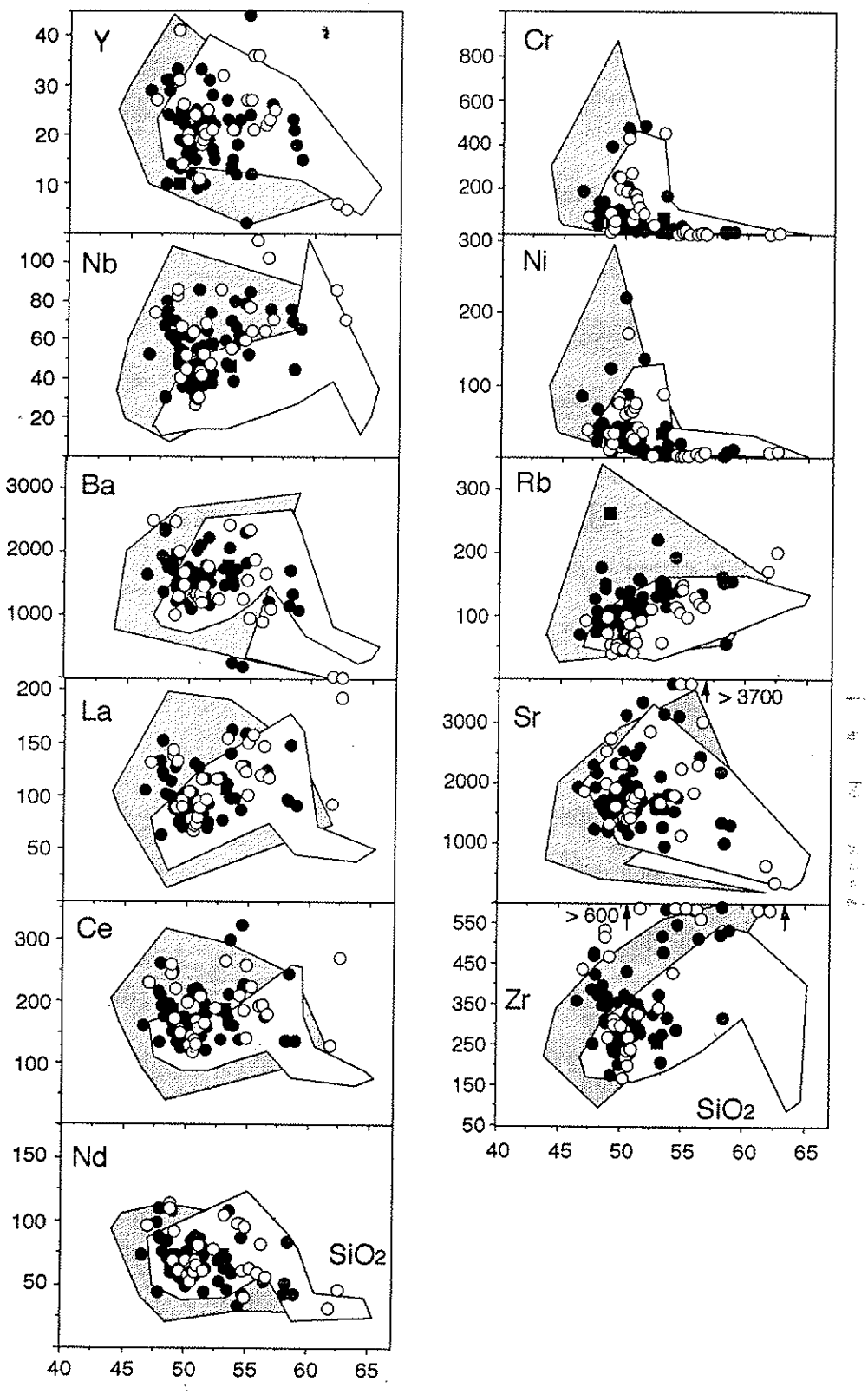

Figure 8B - SiO_2 (wt %) vs. trace (ppm) elements for dykes of the B-T suite. Other symbols as in Fig. 4A.

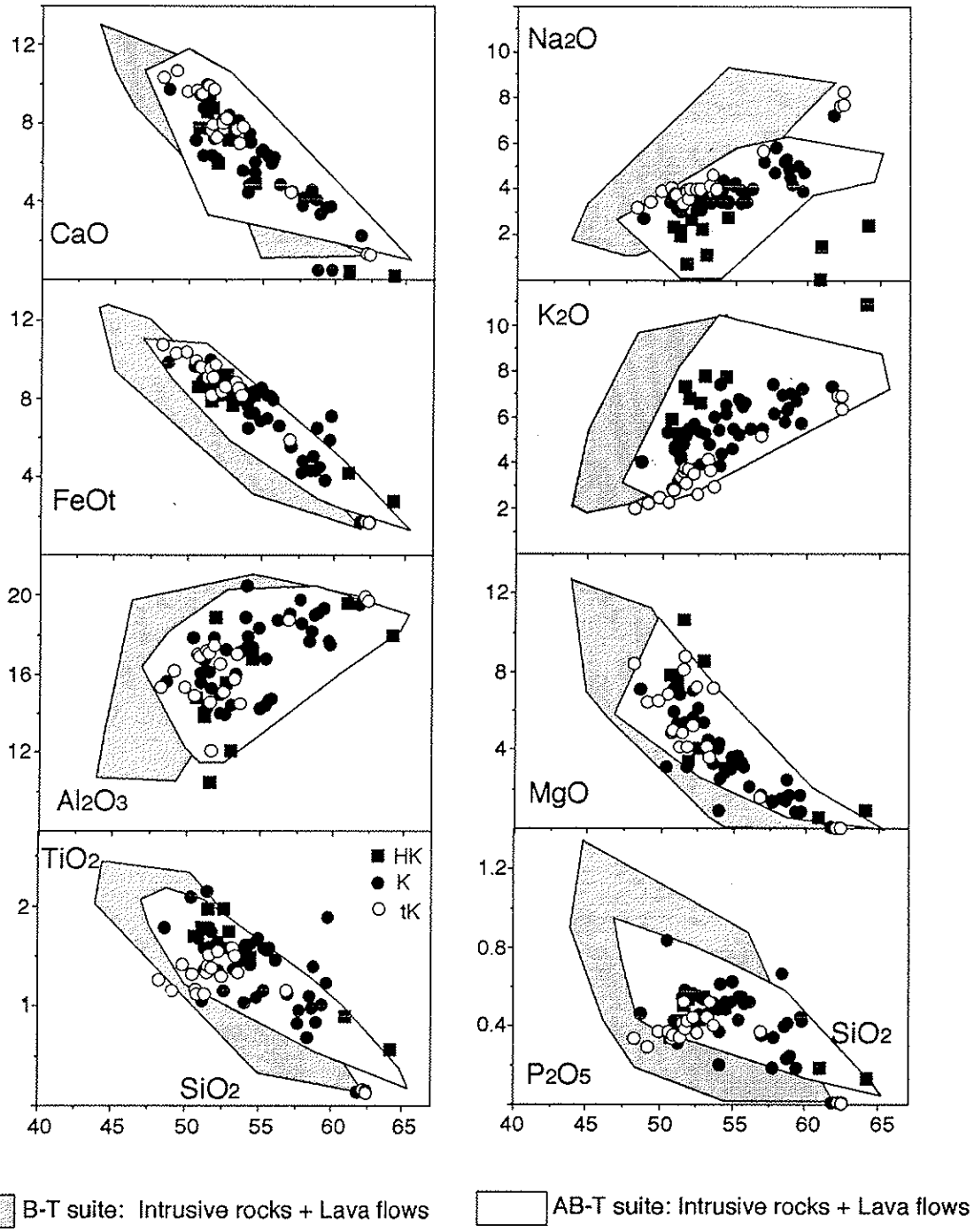

Figure 9A - SiO_2 vs. major elements (wt %) for dykes of the AB-T suite. Symbols as in Fig. 4A.

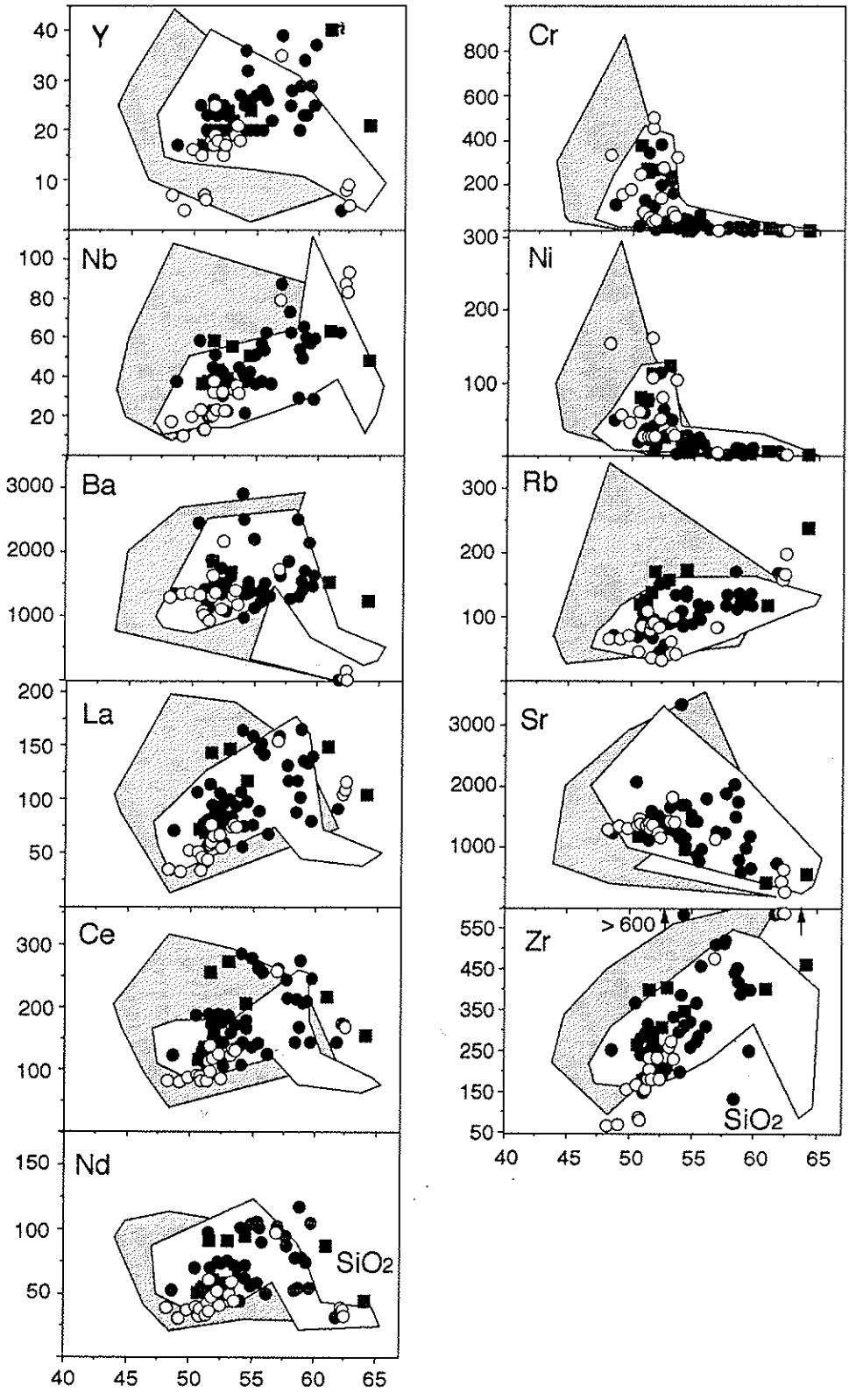

Figure 9B - SiO_2 (wt %) vs. trace (ppm) elements for dykes of the AB-T suite. Symbols, as in Fig. 4A.

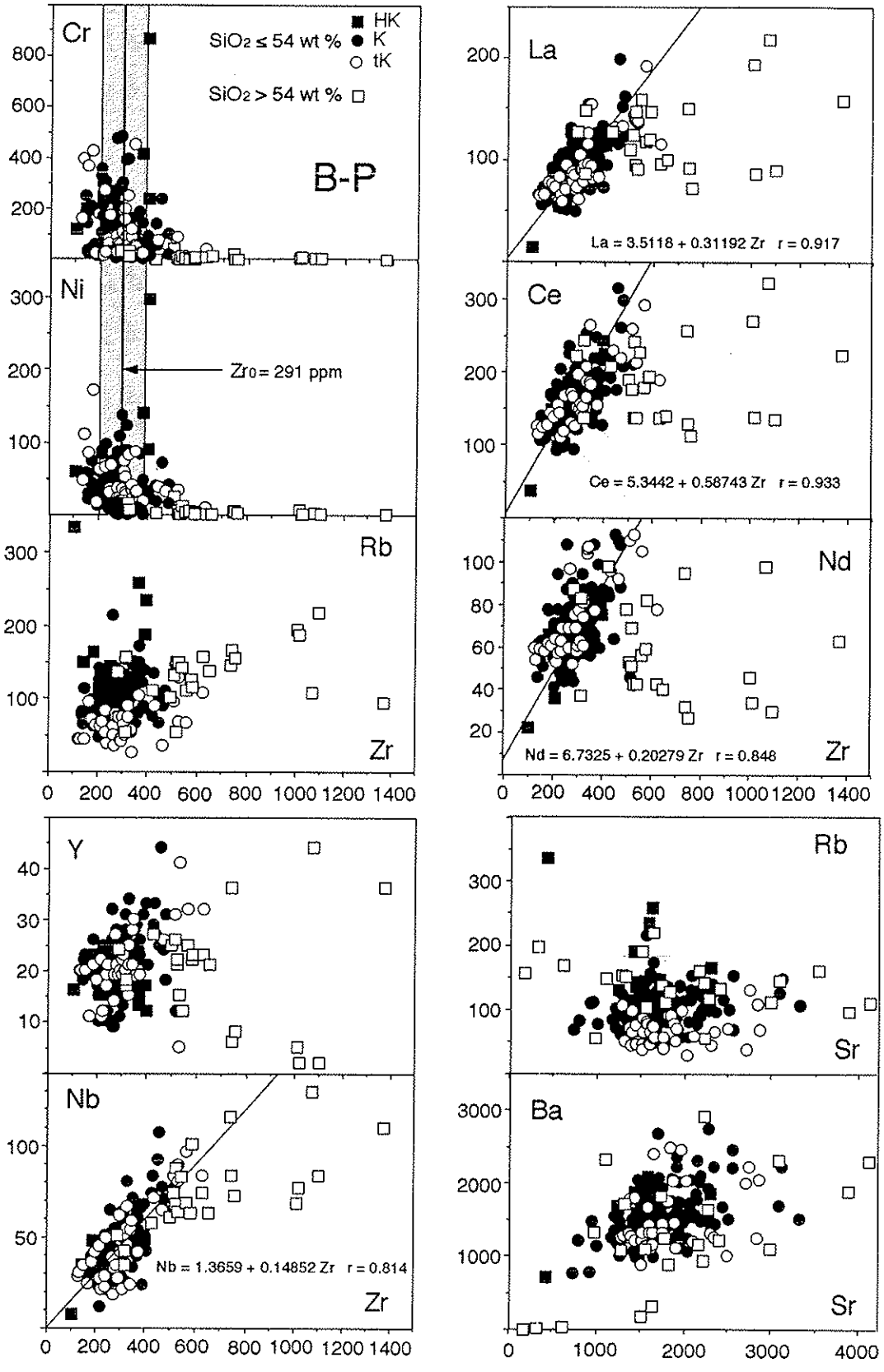

Figure 10 - Zr (ppm) vs. trace (ppm) elements for the B-P suite (intrusive facies+lava flows+dykes).

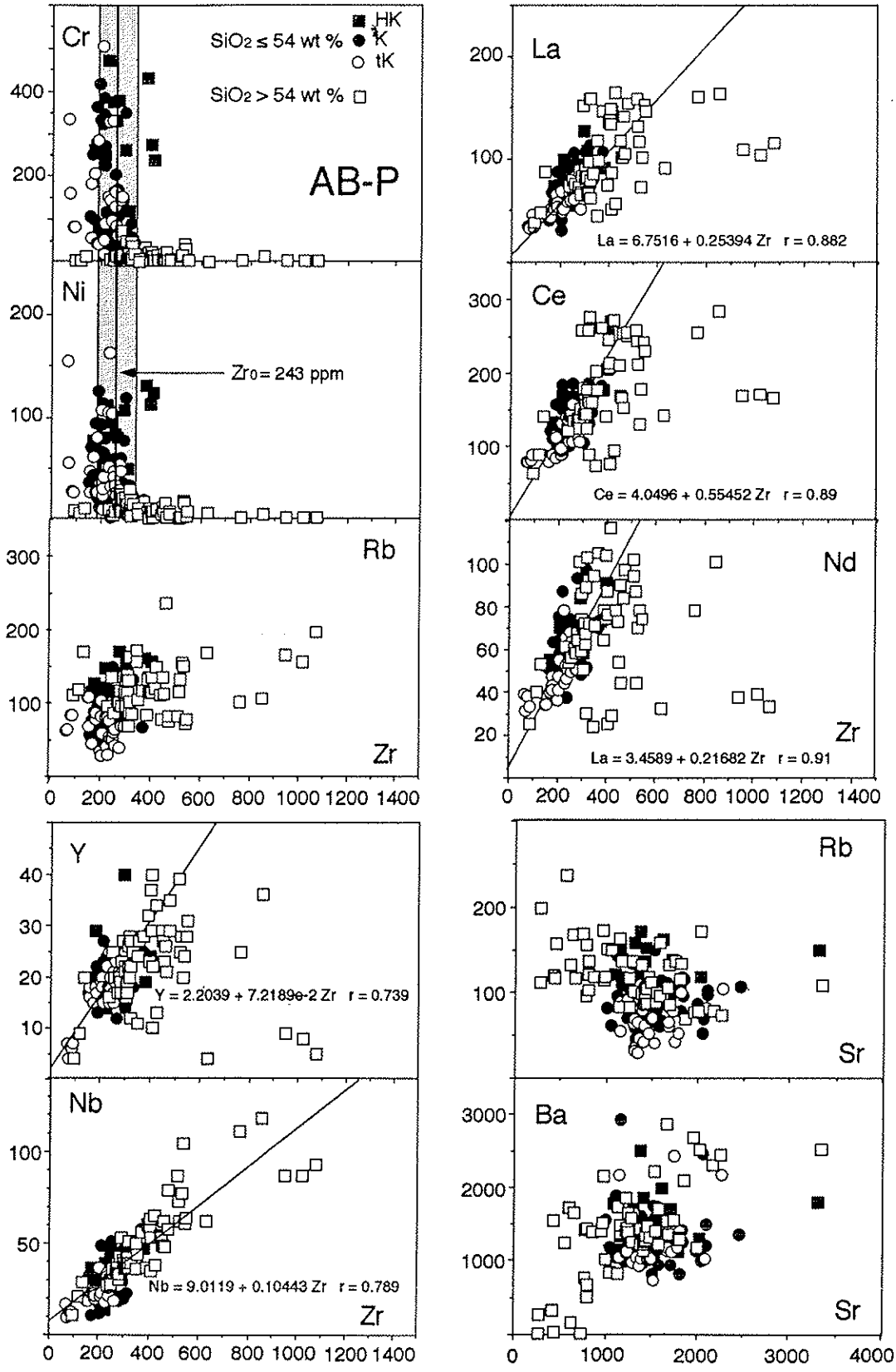

Figure 11- Zr (ppm) vs. trace (ppm) elements for the AB-T suite (intrusive facies+lava flows+dykes).

Table 1-A. Average major (wt %) and trace (ppm) element contents for rocks with $SiO_2 \leq 54$ wt %, B-P suite (standard deviations in parentheses); HK, K, tK: highly potassic, potassic and transitional potassic groups, respectively; N, number of samples.

B-P SUITE

	INTRUSIVE ROCKS				LAVA FLOWS				DYKES				WHOLE
	HK (N=9)	K (N=54)	tK (N=13)	TOTAL (N=77)	HK (N=2)	K (N=31)	tK (N=7)	TOTAL (N=40)	HK (N=2)	K (N=59)	tK (N=19)	TOTAL (N=80)	LINEAGE (N=197)
wt %													
SiO_2	50.29 (2.14)	49.96 (1.91)	49.75 (2.92)	50.08 (2.33)	48.66 (1.61)	50.28 (1.39)	50.01 (1.88)	50.15 (1.49)	51.00 (2.97)	50.33 (2.67)	50.25 (1.41)	50.33 (1.59)	50.20 (1.86)
TiO_2	1.67 (0.19)	1.70 (0.22)	1.77 (0.46)	1.70 (0.28)	1.90 (0.02)	1.63 (0.20)	1.48 (0.44)	1.62 (0.26)	1.70 (0.38)	1.68 (0.32)	1.80 (0.34)	1.71 (0.33)	1.69 (0.30)
Al_2O_3	14.04 (1.60)	15.54 (1.92)	16.19 (1.44)	15.52 (1.91)	14.46 (0.02)	17.17 (1.81)	16.28 (2.76)	16.88 (2.03)	16.08 (0.59)	16.64 (1.89)	15.30 (1.66)	16.31 (1.89)	16.12 (1.93)
FeOt	8.46 (1.25)	9.04 (1.05)	9.29 (1.95)	8.95 (1.38)	9.99 (0.78)	8.89 (1.08)	9.09 (2.15)	9.01 (1.32)	7.88 (0.87)	8.90 (1.32)	9.32 (1.15)	8.97 (1.29)	8.97 (1.33)
MnO	0.15 (0.03)	0.17 (0.02)	0.17 (0.03)	0.17 (0.03)	0.17 (0.02)	0.16 (0.01)	0.17 (0.01)	0.17 (0.01)	0.14 (0.01)	0.17 (0.02)	0.17 (0.02)	0.17 (0.02)	0.17 (0.02)
MgO	6.96 (1.91)	5.70 (1.77)	5.15 (1.74)	5.69 (1.90)	6.27 (0.11)	4.59 (1.46)	5.06 (2.49)	4.76 (1.66)	3.92 (0.06)	4.77 (1.71)	5.61 (1.58)	4.95 (1.69)	5.20 (1.76)
CaO	8.25 (1.98)	8.78 (1.32)	9.12 (1.96)	8.69 (1.70)	9.45 (0.93)	7.69 (1.47)	8.54 (3.11)	7.93 (1.84)	6.90 (0.12)	7.79 (1.52)	8.53 (0.85)	7.95 (1.41)	8.23 (1.61)
Na_2O	2.51 (0.66)	3.55 (0.64)	4.27 (1.05)	3.59 (0.92)	1.76 (0.98)	3.77 (0.61)	4.73 (1.67)	3.84 (1.05)	3.72 (0.11)	3.79 (0.71)	4.62 (0.72)	3.98 (0.79)	3.80 (0.89)
K_2O	7.09 (1.63)	4.90 (0.90)	3.54 (0.97)	4.96 (1.40)	6.14 (0.38)	5.23 (0.75)	4.20 (1.93)	5.10 (1.11)	7.99 (0.93)	5.39 (0.97)	3.80 (0.54)	5.07 (1.20)	5.03 (2.12)
P_2O_5	0.57 (0.23)	0.66 (0.19)	0.74 (0.24)	0.66 (0.21)	0.62 (0.34)	0.54 (0.11)	0.44 (0.19)	0.53 (0.14)	0.68 (0.02)	0.56 (0.16)	0.61 (0.17)	0.57 (0.16)	0.60 (0.18)
ppm													
Rb	175 (71)	98 (20)	64 (21)	108 (62)	145 (19)	104 (19)	71 (30)	101 (27)	203 (81)	109 (31)	68 (21)	101 (38)	103 (49)
Sr	1341 (356)	1639 (352)	1680 (318)	1609 (358)	2199 (161)	1713 (319)	1803 (455)	1753 (350)	1671 (64)	1797 (476)	1832 (104)	1803 (463)	1722 (440)
Zr	256 (36)	273 (69)	286 (55)	273 (72)	224 (52)	259 (55)	252 (144)	286 (75)	310 (78)	308 (74)	332 (125)	314 (88)	291 (88)
Y	16.5 (7.8)	21.1 (5.6)	22.3 (4.0)	21.5 (5.1)	19.5 (4.9)	19.3 (4.22)	16.1 (5.9)	18.8 (4.6)	17.5 (6.4)	20.7 (5.7)	22.1 (7.3)	21.0 (6.1)	21 (6)
Nb	38 (13)	41 (17)	36 (12)	40 (16)	44 (7)	44 (9)	43 (23)	44 (12)	54 (11)	51 (14)	54 (18)	52 (15)	45 (17)
Ba	1563 (129)	1470 (425)	1357 (334)	1463 (406)	1695 (226)	1578 (245)	1481 (456)	1566 (286)	1855 (112)	1527 (333)	1550 (458)	1540 (363)	1523 (392)
La	83 (36)	89 (27)	82 (9)	87(26)	83 (0)	92 (14)	85 (32)	90 (18)	103 (6)	96 (22)	103 (27)	98 (23)	92 (25)
Ce	158 (67)	161 (42)	153 (20)	159 (42)	140 (13)	161 (24)	143 (40)	157 (27)	187 (1)	168 (36)	181 (46)	171 (38)	162 (40)
Nd	60 (20)	72 (14)	75 (19)	68 (16)	64 (4)	67 (12)	57 (10)	65 (12)	68 (7)	68 (15)	75 (19)	70 (16)	68 (16)

Table 1-B. Average major (wt %) and trace (ppm) element contents for rocks with $SiO_2 \leq 54$ wt %, AB-T suite (standard deviations in parentheses); HK, K, tK: highly potassic, potassic and transitional potassic groups, respectively; N, number of samples.

	AB-T SUITE												
	INTRUSIVE ROCKS				LAVA FLOWS				DYKES				WHOLE
	HK (N=5)	K (N=32)	tK (N=8)	TOTAL (N=45)	HK (N=4)	K (N=11)	tK (N=9)	TOTAL (N=24)	HK (N=7)	K (N=19)	tK (N=16)	TOTAL (N=42)	LINEAGE (N=111)
wt %													
SiO_2	52.08 (0.87)	51.21 (1.98)	50.69 (1.22)	51.22 (1.80)	52.19 (1.43)	51.71 (1.53)	50.52 (1.08)	52.09 (1.35)	51.74 (1.84)	51.97 (1.34)	51.38 (2.24)	51.71 (1.33)	51.59 (1.52)
TiO_2	1.54 (0.18)	1.58 (0.24)	1.75 (0.14)	1.60 (0.23)	1.76 (0.26)	1.52 (0.14)	1.39 (0.13)	1.51 (0.20)	1.78 (0.14)	1.55 (0.30)	1.33 (0.15)	1.50 (0.28)	1.54 (0.24)
Al_2O_3	14.86 (1.45)	16..73 (1.45)	16.37 (1.74)	16.46 (1.80)	14.89 (2.84)	15.84 (1.75)	16.78 (0.85)	16.03 (1.76)	14.18 (2.67)	16.06 (1.43)	15.75 (1.1)	15.63 (1.77)	16.05 (1.78)
FeOt	7.80 (1.20)	8.58 (1.14)	8.90 (0.68)	8.55 (1.10)	9.03 (0.64)	8.62 (1.03)	8.62 (0.38)	8.69 (0.86)	8.53 (0.64)	8.81 (0.67)	9.30 (0.82)	8.95 (0.77)	8.73 (0.92)
MnO	0.13 (0.02)	0.16 (0.02)	0.16 (0.02)	0.16 (0.02)	0.17 (0.02)	0.16 (0.02)	0.16 (0.02)	0.16 (0.02)	0.16 (0.03)	0.16 (0.02)	0.17 (0.02)	0.16 (0.02)	0.16 (0.02)
MgO	6.83 (2.60)	5.02 (1.43)	5.34 (1.37)	5.27 (1.63)	7.05 (2.16)	5.90 (2.18)	4.93 (0.92)	5.73 (1.88)	7.06 (2.51)	5.19 (1.32)	5.96 (1.68)	5.80 (1.78)	5.57 (1.74)
CaO	7.43 (1.45)	8.39 (1.50)	8.93 (1.86)	8.38 (1.58)	5.70 (2.78)	7.84 (0.89)	7.61 (0.76)	7.39 (1.47)	7.81 (1.08)	7.64 (1.41)	8.77 (1.19)	8.10 (1.35)	8.06 (1.47)
Na_2O	2.40 (0.53)	3.47 (0.61)	3.89 (0.55)	3.43 (1.70)	0.99 (1.20)	3.35 (0.50)	4.07 (0.34)	3.23 (1.22)	1.90 (0.71)	3.42 (0.30)	3.87 (0.35)	3.34 (0.79)	3.35 (1.25)
K_2O	6.38 (1.29)	4.27 (0.74)	3.32 (0.63)	4.33 (1.12)	7.89 (1.89)	4.57 (0.59)	3.48 (0.40)	4.71 (1.74)	6.38 (1.02)	4.71 (0.76)	3.06 (0.64)	4.36 (1.40)	4.42 (1.36)
P_2O_5	0.55 (0.11)	0.60 (0.12)	0.63 (0.12)	0.60 (0.12)	0.54 (0.07)	0.49 (0.06)	0.47 (0.06)	0.49 (0.07)	0.46 (0.07)	0.49 (0.11)	0.40 (0.06)	0.45 (0.10)	0.52 (0.10)
ppm													
Rb	131(24)	90(18)	71 (19)	92 (24)	125 (320)	97 (20)	69 (26)	91 (31)	140 (21)	91 (25)	71 (23)	92 (33)	92 (32)
Sr	2024 (762)	1591 (278)	1719 (303)	1623 (343)	1334 (282)	1417 (385)	1481 (237)	1428 (312)	1335 (92)	1405 (213)	1366 (141)	1379 (171)	1477 (333)
Zr	267 (65)	249 (44)	263 (25)	253 (44)	267 (44)	248 (47)	235 (26)	246 (40)	288 (93)	255 (56)	175 (67)	230 (80)	243 (64)
Y	17.4 (1.9)	19.2 (2.9)	21.8 (3.0)	19.2 (2.9)	26.8 (8.9)	14.0 (4.0)	18.2 (2.3)	20.0 (5.0)	21.0 (2.5)	221..4 (3.4)	15.1 (6.0)	18.9 (5.3)	19 (5)
Nb	33 (12)	31 (10)	27 (7)	30 (10)	41 (5)	34 (9)	28 (6)	33 (8)	45 (9)	37 (10)	25 (9)	34 (12)	32 (11)
Ba	1532 (356)	1191 (178)	1168 (430)	1234 (278)	1798 (554)	1328 (186)	1254 (45)	1379 (405)	1463 (258)	1535 (475)	1337 (282)	1448 (382)	1354 (405)
La	77 (11)	74 (14)	71 (12)	74 (13)	104 (21)	71 (13)	63 (13)	74 (20)	97 (34)	83 (20)	56 (15)	75 (26)	74 (22)
Ce	138 (30)	136 (21)	132 (17)	135 (21)	162 (9)	129 (21)	115 (19)	129 (24)	171 (63)	143 (33)	102 (21)	132 (43)	132 (34)
Nd	57 (9)	60 (12)	63 (8)	60 (11)	72 (9)	53 (8)	49 (6)	55 (11)	66 (18)	59 (16)	43 (9)	54 (16)	56 (14)

Table 2-A. Concentrations (ppm) of REE, Th, U, Ta, Y (ICPM) and other incompatible elements (XRF) for selected ASU samples (B-P suite); mg#=molecular MgO/(MgO+FeO), assuming $Fe_2O_3/FeO=0.18$.

B-P SUITE

	INTRUSIVE ROCKS							LAVA FLOWS		DYKES						
	1-HK	2-HK	3-HK	4-K	5-K	6-K	7-tK	8-K	9-tK	10-HK	11-HK	12-K	13-K	14-K	15-K	16-tK	17-tK
	51-3152	39-PS530	52-PS264	77-PS245	56-PS268	27-PS535	21-PS539	143-PS31	257-PS-204	D16-501B	D110-PS102	D211-3088	D207-PS111	D213-3398	D151-PS28	D76-PS259	D122-PS34
La	109	21	83	108	106	114	84	88	98	164	98	88	84	63	88	87	106
Ce	196	51	164	204	204	207	153	157	179	302	186	166	140	135	163	162	161
Pr		7.0	18.5	23.8				18.4	20.3	28.8		16.5	15.3		16.2		19.4
Nd	76.5	29.3	66.3	90.2	93.7	84.0	64.8	62.6	74.6	112.4	63.2	60.6	63.8	44.1	55.2	69.5	73.4
Sm	11.3	8.9	11.1	13.8	14.4	12.3	10.12	10.05	12.68	23.5	15.9	14.8	12.80	12.4	13.3	10.80	20.0
Eu	2.88	3.77	3.04	3.67	3.86	3.23	2.76	2.63	3.46	5.6	2.02	2.50	2.38	2.94	2.6	2.95	3.60
Gd	7.46	5.66	5.81	9.09	9.63	7.88	6.89	6.98	8.91	14.5	5.93	6.40	6.40	8.19	6.5	7.09	8.40
Tb		0.75		1.11				0.90	1.06	1.9	0.59	0.75	0.74	1.1	0.90	0.85	0.67
Dy	3.42	3.3	3.79	4.70	4.90	3.96	3.60	4.47	4.88	9.8	2.86	4.05	3.25	4.87	3.61	3.76	3.61
Ho		0.39		1.09				0.79	0.84	1.6		0.68	0.64				0.78
Er	1.55	0.67	1.47	1.77	2.08	1.68	1.67	2.06	2.4	4.4	1.59	1.90	1.80	2.21	2.20	1.54	2.22
Tm		0.05		0.24				0.35	0.29	0.6		0.28	0.23				0.34
Yb	1.07	0.27	1.16	1.36	1.46	1.29	1.35	1.93	1.68	2.2	1.59	1.69	2.00	1.72	1.30	1.17	1.97
Lu	0.2	0.05	0.24	0.24	0.27	0.23	0.26	0.34	0.31	0.13	0.23	0.25	0.20	0.25	0.20	0.20	0.29
Rb	190	337	136	114	69	146	65	128	103	126	260	89	108	72	105	52	69
Ba	1469	715	1741	1958	768	1776	1322	1425	1094	2028	1935	1218	1448	1354	1325	1460	1626
Th	11.32	2.2	6.2	6.6	6.83	13.2	13.8	10.9	24.5	26.9	12.7	13.2	11.3	28.7	10.6	9.5	13.8
U	2.43	0.2	1.9	1.7	1.47	2.5	2.5	2.5	5.8	5.9	3.5	2.6	2.1	6.0	2.3	1.4	2.7
K	48235	78454	48235	44914	16936	58861	36280	48484	34951	54378	68990	33540	38936	30717	41510	28227	27065
Ta	3.5	1.8	2.4	3.1	2.4	4.1	3.9	1.8	4,8	4.0	5.1	3.2	2.2	3.2	3.1	3.6	3.4
Nb	52	12	38	41	34	46	46	48	62	46	62	47	40	30	46	51	52
Sr	1415	437	1507	1624	735	1716	1599	1531	1562	706	1626	1216	1836	1200	1429	1892	1913
P	2444	873	3753	3273	3753	2793	2313	2182	3099	5630	2924	2269	1615	1877	2575	2226	2344
Zr	394	102	252	279	223	254	212	291	498	404	365	303	268	251	278	312	358
Ti	11510	9952	11450	12050	11630	8273	6774	8393	7014	15467	11391	9712	9352	10371	9532	10731	13729
Y	14.5	12.5	18.4	18.8	21.9	17.6	16.9	23.3	15.9	39.0	13.0	15.9	9.2	9.6	17.6	16.6	29.2
Th/Zr	0.0287	0.0216	0.0246	0.0237	0.0306	0.0520	0.0651	0.0375	0.0492	0.0666	0.0348	0.0436	0.0422	0.1143	0.0381	0.0305	0.0386
Nb/Zr	0.1320	0.1177	0.1508	0.1041	0.1525	0.1811	0.2170	0.1649	0.1245	0.1139	0.1699	0.1551	0.1493	0.1195	0.1655	0.1635	0.1453
Th/Yb	10.579	8.148	5.345	4.853	4.678	10.233	10.222	5.648	14.583	12.227	7.987	7.811	5.650	16.686	12.462	8.120	7.001
Ta/Yb	3.271	6.667	2.069	2.279	1.644	3.178	2.889	0.933	5.000	1.818	3.208	1.893	1.100	1.861	2.385	3.077	1.726
mg#	0.695	0.618	0.589	0.683	0.676	0.530	0.506	0.472	0.488	0.512	0.486	0.720	0.628	0.627	0.506	0.605	0.560

Table 2-B. Concentrations (ppm) of REE, Th, U, Ta, Y (ICPM) and other incompatible elements (XRF) for selected ASU samples (AB-T suite); mg#=molecular MgO/(MgO+FeO), assuming $Fe_2O_3/FeO = 0.18$.

AB-T SUITE

	INTRUSIVE ROCKS								LAVA FLOWS				DYKES			
	18-HK	19-K	20-K	21-K	22-K	23-K	24-tK	25-tK	26-tK	27-tK	28-tK	29-tK	30-HK	31-K	32-tK	33-tK
	47-PS263	78-PS243	113-PS228	142-PS30	208-3341	181-3090	103-PS237	259-PS201	199-3344	254-PS206	100-PS233	42-PS315	D159-PS9	D70-PS136B	D97-PS159	D88-PS129
La	108	75	86	71	58	77	63	73	56	52	69	157	81	76	33	35
Ce	197	138	155	130	122	143	120	137	109	101	134	278	119	135	79	88
Pr				13.7	14.7				12.9				13.0			
Nd	65	59.7	65.2	58.2	69.1	59.5	58.2	62.5	52.0	48.8	62.7	97	49.1	56.0	30.8	33.4
Sm	12.9	9.58	10.09	9.75	12.32	9.4	10.05	10.68	8.83	8.45	10.60	14.7	9.8	11.2	9.2	9.7
Eu	2.5	2.62	2.73	2.76	3.72	2.2	2.87	3.07	2.52	2.49	3.00	3.8	2.6	2.73	1.8	2.2
Gd	4.3	6.54	6.79	7.13	8.88	4.6	7.25	7.50	6.16	5.82	7.32	6.6	4.7	6.81	4.2	4.8
Tb				0.85	1.06				0.77				0.65	0.90	0.6	0.7
Dy	3.5	3.46	3.35	4.06	4.82	3.9	3.84	4.51	3.64	3.39	3.85	6.3	3.40	4.69	3.5	4.2
Ho				0.72	0.80				0.65				0.64			
Er	1.2	1.54	1.51	1.97	1.83	1.5	1.65	1.90	1.52	1.50	1.62	3.0	1.70	2.21	1.7	2.0
Tm				0.28	0.26				0.24				0.27			
Yb	1.0	1.14	1.13	1.45	1.41	1.48	1.25	1.69	1.31	1.26	1.30	2.6	1.32	2.30	1.5	2.0
Lu	0.18	0.23	0.21	0.27	0.26	0.21	0.24	0.30	0.23	0.24	0.24	0.4	0.19	0.43	0.17	0.21
Rb	162	123	97	125	53	100	41	70	92	56	81	70	119	88	66	86
Ba	1995	1344	1426	1268	1003	1186	729	1021	1117	1050	1142	2101	1334	1145	1368	1090
Th	9.8	8.4	10.5	6.9	3.4	11.9	6.7	12.4	7.2	8.6	9.1	22	32.2	31.7	2.8	9.6
U	3.1	2.3	2.4	2.2	0.8	2.3	1.7	2.4	1.1	1.4	2.4	5	7.4	9.5	1.4	1.7
K	67495	45578	42838	34370	23910	37525	17932	33125	31797	25736	32295	43254	47487	37359	17600	22416
Ta	3.2	2.5	2.2	1.4	1.8	4.4	1.5	1.9	2.3	1.7	2.5	2	1.1	2.1	1.4	1.2
Nb	48	42	36	26	16	41	28	36	31	27	34	37	37	37	11	14
Sr	1618	1280	1834	1495	2057	1378	1527	1489	1224	1153	1555	1864	1163	1412	1336	1456
P	2575	1833	2575	2880	4059	2182	1615	2924	2051	1571	2400	1397	1484	2269	1266	1397
Zr	282	271	262	213	224	261	282	291	255	239	277	318	268	260	73	91
Ti	10551	10072	7314	10431	12110	7854	10911	9832	9053	8213	9472	5396	9862	6295	6535	6595
Y	19	15.7	15.3	19.2	21.9	18.0	17.5	22.2	17.4	16.0	23.0	28	19.3	20.0	4.2	7.1
Th/Zr	0.0257	0.0310	0.0401	0.0324	0.0152	0.0456	0.0238	0.0426	0.0282	0.0360	0.0329	0.0692	0.1201	0.1219	0.0384	0.1055
Nb/Zr	0.1257	0.1550	0.1374	0.1221	0.0714	0.1571	0.0993	0.1237	0.1216	0:1130	0.1227	0.1164	0.1381	0.1423	0.1507	0.1538
Th/Yb	9.800	7.368	9.292	4.759	2.413	8.041	5.360	7.337	5.496	5.089	7.000	8.462	24.394	13.783	1.867	4.800
Ta/Yb	3.200	2.193	1.947	0.966	1.277	2.973	1.200	1.124	1.756	1.349	1.923	0.769	0.833	0.913	0.933	0.600
mg#	0.651	0.618	0.571	0.541	0.529	0.478	0.625	0.524	0.578	0.524	0.520	0.279	0.652	0.476	0.564	0.510

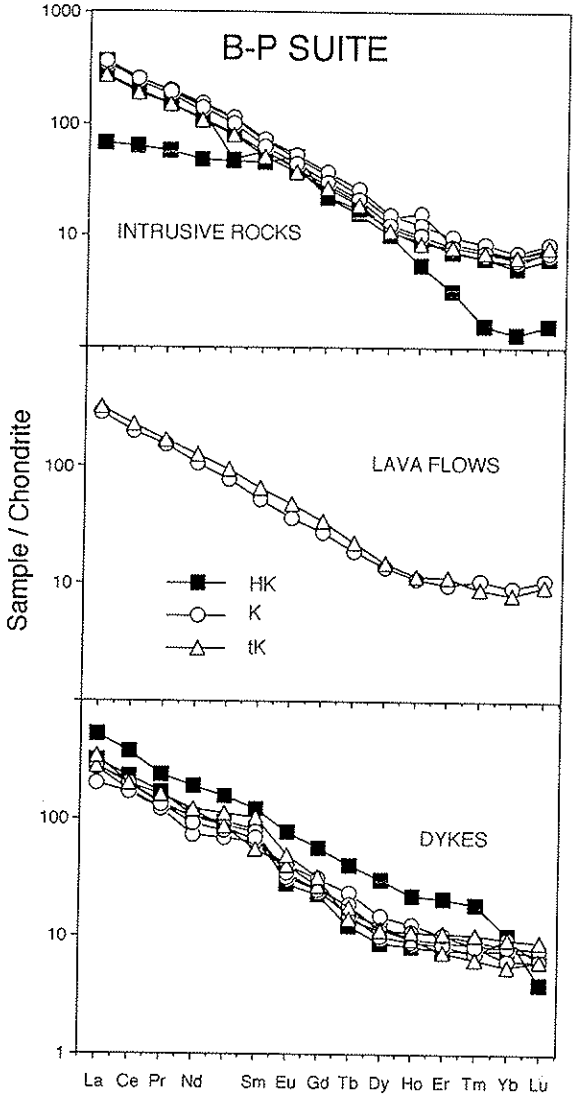

Figure 12 - Chondrite-normalized REE diagram for compositions from the B-P suite. HK, K and tK: highly potassic, potassic and transitional potassic groups, respectively. Normalizing values are from Boynton (1984).

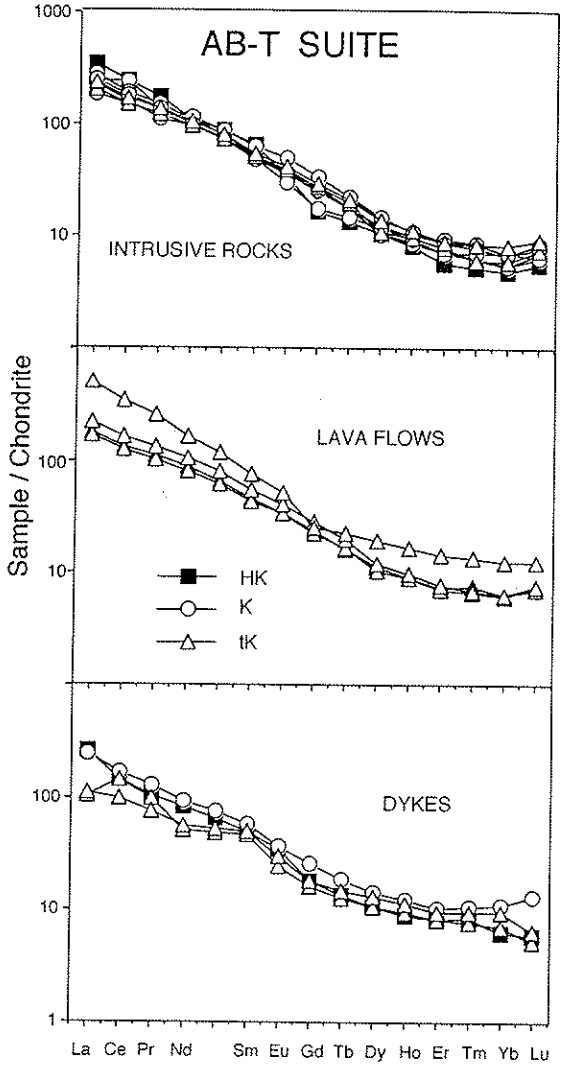

Figure 13 - Chondrite-normalized REE diagram for rocks from the AB-T suite. Symbols as in Fig. 12.

The origin of Eu anomalies has not been satisfactorily explained. Feldspar fractionation, cumulus processes, or mixtures of phenocryst (xenocryst)-loaded liquids from different stages of magmatic evolution (Comin-Chiaramonti et al., 1993) are plausible means for producing slightly deficiency or excess in Eu. However, it should be noted that both anomalies are present in the less evolved potassic compositions (mg#$\geq$0.6, for both groups), suggesting that these anomalies may have also been inherited from the magma source.

The incompatible element-enriched nature of the alkaline magma(s) of the Asunción-Sapucai graben is also apparent from the normalized trace element plots which include some of the REE data (Figs. 14 and 15).

In general, B-P and AB-T compositions have similar element enrichment patterns for large ion lithophile elements (LILE), i.e. Rb, Ba, and other incompatible elements like La, Ce, Sm and Tb. Th and U show relative enrichments in the lavas and dykes, but generally tend to be depleted.

The high-field-strenght elements (HFSE), particularly Ta, Nb and Ti, display marked depletion and yielded negative Ta/Nb-Ti anomalies. These anomalies were generally interpreted (e.g. Pearce, 1983; Thompson et al., 1984; Nelson, 1992) as characteristic of magmas generated in subduction-related environments.

In general, the B-P suite displays higher Ti, K, Zr, Nb, Y and REE contents than those shown by the AB-T one.

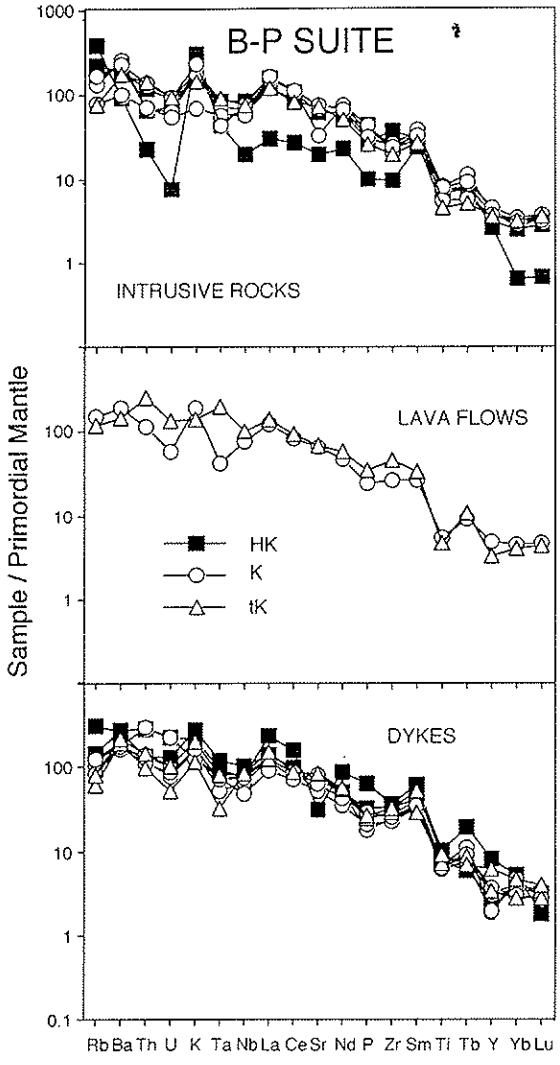

Figure 14 - Primordial mantle-normalized trace element data for selected specimens of the B-P suite. Normalizing values are from Wood et al. (1979).

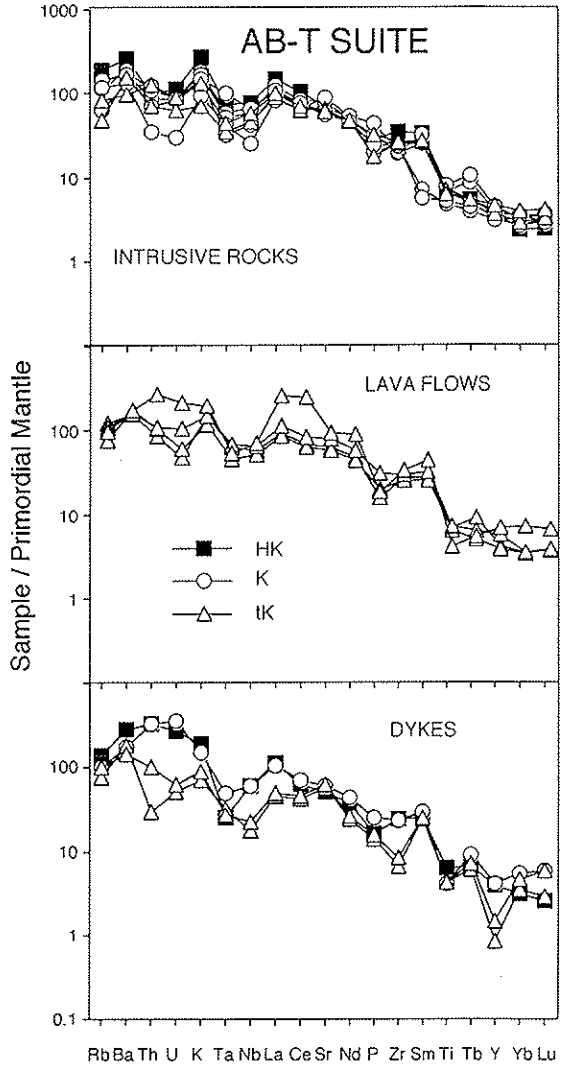

Figure 15 - Primordial mantle-normalized trace element data for selected specimens of the AB-T suite.

Notably, the IE variations of the potassic suites from the Asunción-Sapucai graben essentially mimic those of the associated tholeiitic basalts (Serra Geral Formation), and contrast the behaviour of the sodic suites characterized by strong Ta-Nb positive spikes (Fig. 16).

CONCLUDING REMARKS

The ASU province as a whole exhibits a wide range in composition, where intrusives, lavas and dykes display similar petrochemical variations. This probably reflects similar parental magmas. The dykes may have been potential feeders for the potassic magma(s).

All compositions representative of the less evolved magmas (mg# 0.63-0.73) yielded low Cr and Ni, indicating that they are likely to be derivative of more "primitive" compositions (Green, 1971; Sato, 1977).

The variation diagrams show large scatter and the observed trends are indicative of complex petrogenetic processes, combined with fractional crystallization, in the evolution of the Paraguay magmas.

Chondrite-normalized REE patterns display strong HREE fractionation, supporting a garnet peridotite mantle sources both for the B-P and AB-T suites.

Hygromagmatophile element patterns show strong LILE/HFSE fractionation and negative Ta-Nb and Ti spikes that parallel those of the associ-

ated tholeiitic flood basalts of the Serra Geral Formation.

Therefore, the popular interpretation that similar Ta-Nb, and Ti anomalies for HKS suites elsewhere indicate a subduction-driven magma genesis (e.g. Roman Region Lavas; cf. Civetta et al., 1987, and Beccaluva et al., 1991) is not applicable to the Paraguay alkaline province. Notably, the Tertiary sodic suites spatially associated with the ASU potassic rocks, shows strong Ta-Nb positive spikes (cf. Comin-Chiaramonti et al., 1992).

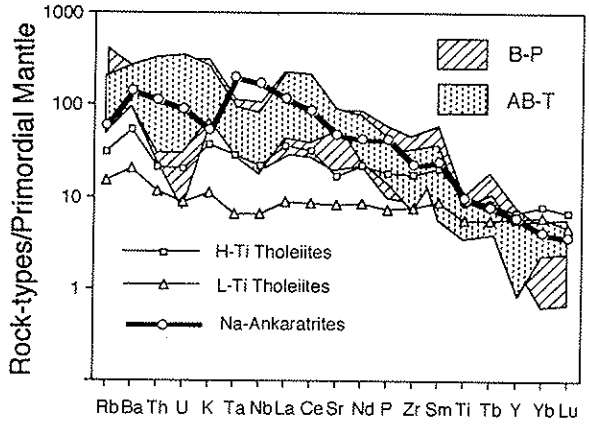

Figure 16 - Primordial mantle-normalized trace element data for B-P and AB-T suites, compared with high-Ti (H-Ti) and low-Ti (L-Ti) Paraná tholeiites and ASU Na-suites. Data sources: Comin-Chiaramonti et al. (1991, 1992).

ACKNOWLEDGEMENTS

Thanks are due to Brazilian (FAPESP) and Italian (CNR and MURST) agencies and to the Universities of Trieste and São Paulo for financial supports.

REFERENCES

ALAIMO, R. & CENSI, P. (1992) Quantitative determination of major, minor and trace elements in USGS rock standards by inductively coupled plasma-mass spectrometry. Atomic Spectroscopy, *13*:113-117.

BECCALUVA, L.; DI GIROLAMO, P.; SERRI, G. (1991) Petrogenesis and tectonic setting of the Roman Volcanic Province, Italy. Lithos, *26*:191-221.

BELLIENI, G.; BROTZU, P.; COMIN-CHIARAMONTI, P.; ERNESTO, M.; MELFI, A.J.; PACCA, I.G.; PICCIRILLO, E.M.; STOLFA, D. (1983) Petrological and paleomagnetic data on the plateau basalt to rhyolite sequences of the southern Paraná Brazil. An. Acad. brasil. Ciênc., *55*:355-383.

BELLIENI, G.; COMIN-CHIARAMONTI, P; MARQUES, L.S.; MARTINEZ, L.A.; MELFI, A.J.; NARDY, A.J.R.; PICCIRILLO, E.M.; STOLFA, D (1986) Continental flood basalts from the central-western regions of the Paraná plateau (Paraguay and Argentina): petrology and petrogenetic aspects. Neues Jb. Miner. Abh., *154*:111-139.

BOYNTON, W.V. (1984) Cosmochemistry of the rare earth elements: meteorite studies. In: P. Henderson (ed.) Rare element geochemistry Elsevier Publ. Co, Amsterdam, p. 63-114.

CIVETTA, L.; FRANCALANCI, L.; MANETTI, P.; PECCERILLO, A. (1987) Petrological and geochemical variations across the Roman Comagmatic Province: inference on magma genesis and crust-mantle evolution. Accad Lincei, *86*:250-269.

COMIN-CHIARAMONTI, P.; CIVETTA, L.; PETRINI, R.; PICCIRILLO, E.M.; BELLIENI, G.; CENSI, P.; BITSCHENE, P.; DEMARCHI, G.; DE MIN, A.; GOMES, C.B.; CASTILLO, A.M.C.; VELÁZQUEZ, J.C. (1991) Tertiary nephelinitic magmatism in Eastern Paraguay: petrology, Sr-Nd isotopes and genetic relationships with associated spinel-peridotite xenoliths. Eur. J. Mineral., *3*:507-525.

COMIN-CHIARAMONTI, P.; CUNDARI, A.; GOMES, C.B.; PICCIRILLO, E.M.; CENSI, P.; DE MIN, A.; BELLIENI, G.; VELÁZQUEZ, V.F.; ORUÉ, D. (1992) Potassic dyke swarm in the Sapucai graben, Eastern Paraguay: petrographical, mineralogical and geochemical outlines. Lithos, *28*: 283-301.

COMIN-CHIARAMONTI, P.; GOMES, C.B.; CENSI, P.; DE MIN, A.; ROTOLO, S.G.; VELÁZQUEZ, V.F. (1993) Geoquímica do magmatismo pós-paleozóico no Paraguai Centro-Oriental. Geochim. Brasil., *7*:19-34.

COMIN-CHIARAMONTI, P.; CUNDARI, A.; BELLIENI, G. (this volume) Mineral chem-

istry of alkaline rocks from the Asunción-Sapucai graben. Appendix III.

COMIN-CHIARAMONTI, P; CUNDARI, A.; DE MIN, A; GOMES, C.B.; VELÁZQUEZ, V.F. (this volume) Magmatism in Eastern Paraguay: occurrence and petrography.

COMIN-CHIARAMONTI, P.; DE MIN, A.; MARZOLI, A. (this volume) Magmatic rock-types from the Asunción-Sapucai graben: chemical analyses. Appendix II.

CUNDARI, A. & COMIN-CHIARAMONTI, P. (this volume) Mineral chemistry of alkaline rocks from the Asunción-Sapucai graben (central-eastern Paraguay).

DE LA ROCHE, H.; LETERRIER, J.; GRANDCLAUDE, P.; MARCHAL, M. (1980) A classification of volcanic and plutonic rocks using R1-R2 diagram and major element analyses. Its relationships with current nomenclature. Chem. Geol., *29*:183-210.

GOMES, C.B.; COMIN-CHIARAMONTI, P.; VELÁZQUEZ, D.; ORUÉ, D. (this volume) Alkaline magmatism in Paraguay: a review.

GREEN, D.H. (1971) Composition of basaltic magma as indicators of conditions of origin: application to oceanic volcanism. Phi. Trans. R. Soc. London, *A268*:707-725.

NELSON, D.R. (1992) Isotopic characteristics of potassic rocks: evidence for the involvement of subducted sediments in magma genesis. Lithos, *28*:403-420.

PEARCE, J.A. (1983) Role of the sub-continental lithosphere in magma genesis at active continental margins. In: C.J. Hawkesworth & M.J. Norry (eds.) Continental basalts and mantle xenoliths. Shiva, Nantwitch, p.230-249.

SATO, H. (1977) Nickel content of basaltic magmas; identification of primary magma as a measure of the degree of olivine fractionation. Lithos, *10*:113-120.

THOMPSON, R.N.; MORRISON, M.A.; HENDRY, G.L.; PARRY, S.J. (1984) An assessment of the relative roles of crust and mantle in magma genesis: an elemental approach. Phil. Trans. R. Soc. London, *A310*: 549-590.

WOOD, D.A.; TARNEY, J; VARET, J.; SAUNDERS, A.D.; BOUGAULT, H.; JORON, J.L.; TREUIL, M.; CANN, J.R. (1979) Geochemistry of basalts drilled in the North Atlantic by IPOD Leg 49: implications for mantle heterogeneity. Earth Planet. Sci. Lett., *42*:77-97.